Applied Mathematical Modelling 44 (2017) 336–356

Contents lists available at ScienceDirect

Applied Mathematical Modelling

journal homepage: www.elsevier.com/locate/apm

A smart displacement based (SDB) beam element with distributed plasticity

B. Pantò*, D. Rapicavoli, S. Caddemi, I. Caliò

Dipartimento Ingegneria Civile e Architettura, Università degli Studi di Catania, Via Santa Sofia 64, 95123 Catania, Italy

ARTICLE INFO

Article history:
Received 12 July 2016
Revised 24 November 2016
Accepted 5 January 2017
Available online 11 January 2017

Keywords:
Non-linear analysis
Finite element method
Generalised functions
Plastic beam element
Displacement shape functions
Smart Displacement Based (SDB) element

ABSTRACT

The standard displacement based inelastic beam element suffers of approximations related to the inability of the cubic polynomial interpolation functions to properly describe the displacement response of the beam when exhibiting inelastic behaviour. The increase of the number of finite elements, or the use of higher order functions with additional internal degrees of freedom, are common remedies suggested to improve the approximation leading to an unavoidable reduction of the computational efficiency. Alternatively, it has been shown that the development of force based finite elements, based on the adoption of exact force shape functions, lead to more accurate results, although requiring different and more complicated iterative solution strategies. Within this scenario, this paper proposes a new inelastic beam element, within the context of the displacement based approach, based on variable displacement shape functions, whose analytic expressions are related to the plastic deformation evolution in the beam element. The adaptive generalised displacement shape are obtained by identifying, at each step, an equivalent tangent beam, characterised by abrupt variations of flexural stiffness, as a suitable representation of the current inelastic state of the beam. The presented approach leads to the formulation of a Smart Displacement Based (SDB) beam element whose accuracy appears to be comparable to those obtained through a force based approach but requiring a reduced implementation effort and a more straightforward approach. The term 'smart' aims at emphasizing the ability of the element to upgrade the displacement field according to the current inelastic state.

1. Introduction

The most diffused computational models for the linear and nonlinear, elastic and inelastic, beam bending problems rely on a discretisation of the one-dimensional continuous beam by means of finite elements. Since the initial proposition of the finite element basic idea, the specific literature on the subject developed, with particular attention, both to theoretical and computational aspects also due to the parallel dramatic progression of the hardware computer facilities. The novelties relevant to this topic are still numerous and testify to the current interest both in the scientific community and in the professional practice. The latter aspect is particularly supported by the implementation into new commercial codes, as well as frequent updating of existing codes, by the numerous software houses and academic research groups.

* Corresponding author.
E-mail address: bpanto@dica.unict.it (B. Pantò).

http://dx.doi.org/10.1016/j.apm.2017.01.018

Besides being outside of the scope of the present paper, the authors feel in awe to even mention the great amount of the literature on the subject or else to choose the most representative piece of work. Hence, the introductory choice to clarify the precise context, framing the new idea presented in this work, is made.

According to the displacement formulation, a beam finite element is defined by means of polynomial interpolation functions, suitably chosen to approximate the displacement field along the beam span [1–6]. The latter choice affects the shape into which the element can be deformed and gives rise to the so-called shape functions able to describe, according to the compatibility relations, the strain components and, furthermore, leads to the definition of the stiffness matrix of the discretised structure.

It is generally recognised that displacement based (DB) finite elements are conceptually simple and easy to implement, however, they are affected by severe approximation, particularly when inelastic analysis has to be performed. When plastic deformations are involved, accurate results can be achieved by a discretisation of each structural member into several finite elements (mesh refinement) or by the introduction of higher order displacement shape functions. In both cases, a good approximation leads inevitably to an increasing number of degrees of freedom and a consequent reduction of the computational efficiency. The DB finite element approach is also named “stiffness approach” since the element stiffness matrix is directly derived by the adopted displacement shape functions.

Despite the initial popularity of DB finite elements, better accuracy in the inelastic analysis of structures have been successfully obtained by making use of force based (FB) models where the exclusive adoption of force shape functions is introduced. In fact, force shape functions, describing the internal force distribution, are prone to account for the along span distributed load and represent the exact solution of the governing equilibrium equations irrespective of the occurrence of plastic deformations. On the basis of the adopted force shape functions the flexibility matrix of the discretised structure is built, so that the method is also addressed to as “flexibility approach”.

One of the first implementations of the FB approach can be found in [7,8]. However, further advances on the method are contained in [9,10]. One of the reasons that refrained the popularity of the FB approach was due to rare availability of sectional constitutive laws in terms of flexibility, rather that stiffness matrix. Furthermore, implementing the FB finite element into codes based on the stiffness method, required an additional inner iterative procedure to determine the element resisting forces [11]. The latter disadvantage has been somehow avoided by introducing a vector of residual displacements, in connection with the usual unbalanced forces, that gives rise to additional residual forces to be accounted for in the global equilibrium equations [12].

The FB approach has been also implemented to define a fibre beam element where the sectional constitutive law is avoided and, rather, the nonlinear constitutive behaviour is remitted to uniaxial fibres into which the section is discretised [13,14]. The fibre beam element is particularly suitable for reinforced concrete sections [15,16]. Subdivision of the cross section into fibres, or layers, although with significant increment of the computational effort with regard to the cross section analysis, it delivers accurate results. Differently from the DB approach, it has to be pointed out that in the FB finite elements no interpolation for displacements is needed hence the knowledge of the displacement field within the element is not straightforward. Since in the FB approach deformations are monitored at integration points, to reconstruct the displacement field a methodology has been developed to interpolate the displacements in terms of curvature at the integration points, relying on a double integration, named Curvature-Based Displacement Interpolation (CBDI) [17].

Approaches based on independent interpolation of forces and displacements have been addressed to as “mixed methods” so as to capture the advantages of both stiffness and flexibility formulations [18–20]. In most cases the mixed approach is adopted for applications with displacement dependent equilibrium equations. Differently from other proposed approaches [21,22] a full variationally consistent mixed method, based on the Hu–Washizu principle, has been proposed in [23] both for elastic and inelastic analysis of beam-like and frame structures. Precisely, internal forces approximations, satisfying equilibrium, are introduced together with discontinuous strain approximations, while, for static applications, no displacement interpolation is needed, being the latter expressed in terms of nodal values.

Within the framework of the mixed approaches, the procedure of Taylor et al. [23] is appealing since with a reduced computational effort delivers accurate results, comparable to FB methods, by avoiding cumbersome mesh refinement.

Bearing in mind the differences highlighted between the mentioned approaches, it can generally be stated that, towards acquisition of more accurate results, DB models require a mesh refinement while FB may act on increasing the number of Gauss points to improve the integration of the inelastic constitutive behaviour while leaving unaltered the structural discretisation (i.e. one finite element each structural member).

For the latter reason the classical DB approach requires huge computational effort and modelling demands that makes it unsuitable for the nonlinear analysis of real structures. With this regard the application of nonlinear adaptive analysis techniques (i.e. automatic mesh refinement) have been proposed in the literature for the analysis of steel frames [24,25] and reinforced concrete frames [26,27]. The latter approach makes use of a powerful quartic formulation in the elastic range capable of representing a single entire beam member with one element. Successively, during analysis, all the structural members are checked for the development of material inelasticity and automatic refined subdivision of quartic elements, in the inelastic zones into elasto-plastic cubic elements, is performed to account for the diffusion of plasticity across the section depth and along the element length. The accuracy and efficiency of the adaptive analysis is verified through applications using the nonlinear analysis program ADAPTIC [28] providing comparisons with results of existing analysis methods for reinforced concrete frames to illustrate the advantages of the adaptive mesh refinement DB approach.

The need of a drastic improvement of the classical DB finite element model for the inelastic analysis of beam-like and frame structures is the main motivation of this work. The intention is to show that an improvement of the accuracy of the DB approach, for inelastic analysis of structures, can be pursued without finite element mesh refining, however, by leaving unaltered the simplicity of the standard approach. Precisely, the construction of new displacement shape functions, to be updated according to the post-yielding stiffness reduction, is proposed.

Borrowing the terminology proposed by Izzudin and co-workers, “adaptive shape functions” rather than “adaptive mesh” is used in this work. To the authors’ knowledge, the only precedent can be found in [29] where flexibility dependent shape functions are updated during the inelastic analysis with a numerical procedure based on inversion of the flexibility matrix at each iteration. On the contrary, the shape functions to be updated are proposed in this work under explicit closed form expressions that do not require additional computational work.

The above displacement shape function updating is built in the iterative procedure of the Newton–Raphson type and leads to enriched forms of the structural stiffness matrix and internal as well as external nodal forces. In the proposed displacement shape functions the stiffness degradation due to the occurrence of inelastic deformations is accounted for, according to a stepwise distribution, for the description of the displacement field. Namely the closed form solution, expressed in terms of generalised functions, of a multi-stepped beam element is adopted for the description of the displacement field of the beam, as a function of its current inelastic behaviour. The resulting adaptive beam element will be addressed to as Smart Displacement Based (SDB) element, where the term ‘smart’ is related to the ability of the element to upgrade the displacement field consistent with its inelastic state.

The proposed SDB element is able to follow closely the diffusion of plasticity by also including the effect of the distributed external load providing the final displacement field with no additional iterations and is straightforwardly implementable into existing displacement based finite element codes.

The results of the proposed procedure have been tested for beam structures for which exact closed form solutions, describing diffusion of plastic deformations along the axis, are available in the literature [30]. In latter case a cross sectional moment curvature constitutive law, inferred by progressive yielding of the cross sections fibres, is considered. Furthermore, a comparison for a case of an inelastic beam with hardening with the appealing mixed approach proposed in [23] is also presented.

2. The multi-stepped linear beam element

The standard displacement based inelastic beam element suffers of approximations related to the inability of the standard cubic polynomial interpolation function to properly describe the displacement response of the beam when exhibiting inelastic behaviour. The occurrence of diffused plastic deformations, along a beam element, is source of abrupt variation of curvature in those portions of the beam when the plastic deformations occur. As a consequence the assumption of a invariable polynomial interpolation function, during the inelastic analysis, is source of approximations that is generally solved by increasing the number of element and/or by considering higher order functions with additional degrees of freedom. From a theoretical point of view, the availability of an accurate solution of the displacement function of the beam undergoing inelastic deformation could allow to maintain the advantages offered by the displacement based approach without the need to increase the number of element and, as a result, the computational demand. To obtain such a result, the exact explicit solution of a beam model undergoing abrupt changes of flexural stiffness in a linear context is here proposed as the starting point for the formulation of a beam finite element able to account for the occurrence of diffused plasticity. For the latter reason, first, in this section we lay the bases for the formulation of an inelastic one dimensional finite element by briefly recalling a model of the elastic Euler-Bernoulli beam characterised by multiple abrupt changes of the flexural stiffness [31,32]. Besides the mentioned plastic deformations, abrupt changes of the flexural stiffness might also be caused by change of material or of the cross-section or else by the occurrence of damage. The presence of a certain number of steps in such beams has led to the denomination of “stepped beams”. The latter beams can be studied by means of classical approaches based on enforcement of transition conditions at the discontinuous cross sections (requiring the introduction of four additional integration constants for each discontinuity). Alternatively, a more convenient approach based on the so called transfer matrix approach has been proposed [33,34]. The linear problems of beams in presence of singularities has been treated successfully by means of the use of distributions, both in static [35–38] and dynamic context [39–41]. The latter distributional approach led to the formulation of a linear beam finite element able to account for different types of singularities also by adopting the classical Timoshenko theory to account for the shear deformations [42–45].

In this section we will consider the distributional approach based on the integration of the governing equation over a single integration domain (beam span) by making use of the theory of generalised functions (distributions) to embed the cross section discontinuities.

The generalised function approach leads to convenient closed form solutions formulated in terms of ‘four’ integration constants only depending solely on the end boundary conditions and independent of the along axis discontinuities. Furthermore, the abrupt changes of elastic flexural stiffness considered in this section will be treated, in the following sections, as representative of the flexural stiffness reduction due to the occurrence of plastic deformations over a specified beam segment.

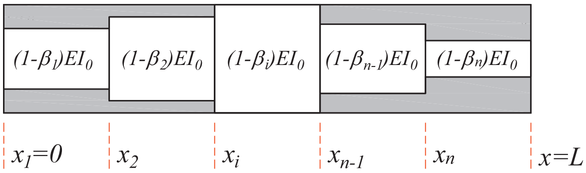

Fig. 1. A multi-stepped beam.

The distributional model for the flexural stiffness $EI(x)$ of a multi-stepped beam, as depicted in Fig. 1, slightly rearranged with respect to that proposed in [32], therein used for a linear analysis, is as follows:

$$EI(x) = EI_o\left[1 - \sum_{i=1}^{n}(\beta_i - \beta_{i-1})U(x - x_i)\right] \tag{1}$$

characterised by n abrupt changes of intensity $\beta_i - \beta_{i-1}$ at abscissas x_i, applied to an initial reference value EI_o, where $U(x - x_i)$ is the Heaviside (unit step) generalised function. The multi-stepped beam model introduced in Eq. (1) implies that the beam is composed of n segments with flexural stiffness EI_i, $i = 1, \ldots, n$, by assuming $\beta_i = \frac{EI_o - EI_i}{EI_o}$.

In particular, the summation term containing the Heaviside function may account for cross-section or material variations or else, alterations of the flexural stiffness accounting for non linear inelastic behaviour caused by the occurrence of irreversible plastic deformations in a specified beam segment. In the latter case the parameters β_i have to be considered as variables to be updated according to a chosen plastic constitutive law. Precisely, the values of the parameters β_i are inferred, later in this work, according to the proposed iterative procedure in such a way that the differences $\beta_i - \beta_{i-1}$ are associated to the flexural stiffness change due to the adopted bending moment-curvature cross-section plastic constitutive law.

The fourth order static governing equation of the multi-stepped Euler-Bernoulli beam subjected to a transversal load $\bar{p}(x)$ distribution, accounting for the spatial variable flexural stiffness $EI(x)$ as defined in Eq. (1), is written as follows:

$$EI_o\frac{d^2}{dx^2}\left\{\left[1 - \sum_{i=1}^{n}(\beta_i - \beta_{i-1})U(x - x_i)\right]\frac{d^2}{dx^2}v(x)\right\} = \bar{p}(x) \tag{2}$$

where $v(x)$ is the transversal deflection function.

The governing Eq. (2) can be conveniently given a non dimensional form, by considering the dimensionless coordinate $\xi = x/L$ (being L the beam length), as follows:

$$\left[\left[1 - \sum_{i=1}^{n}(\beta_i - \beta_{i-1})U(\xi - \xi_i)\right]u^{II}(\xi)\right]^{II} = p(\xi) \tag{3}$$

where the apex indicates the differentiation with respect to ξ.

Eq. (3) is expressed in term of the normalised deflection function $u(\xi) = \frac{v(\xi)}{L}$ and the normalised transversal load parameter $p(\xi) = \frac{\bar{p}(\xi)}{EI_o}L^3$.

The procedure to derive the closed form expression of the normalised governing Eq. (3) can be initiated by a straight double integration as follows:

$$u^{II}(\xi) = \frac{1}{1 - \sum_{j=1}^{n}(\beta_i - \beta_{i-1})U(\xi - \xi_i)}\left[p^{[2]}(\xi) + b_1\xi + b_2\right] \tag{4}$$

where b_1, b_2 are integration constants and $p^{[k]}(\xi)$ indicates the kth primitive function of the external load $p(\xi)$, namely $p^{[1]}(\xi) = \int_0^{\xi} p(s_1)ds_1$, $p^{[2]}(\xi) = \int_0^{\xi}\int_0^{s_1} p(s_2)ds_2ds_1$, and so on.

In view of the well known properties of the Heaviside generalised function, Eq. (4) can also be written as follows:

$$u^{II}(\xi) = \left[1 + \sum_{i=1}^{n}\beta_i{}^{*}U(\xi - \xi_i)\right]\left[p^{[2]}(\xi) + b_1\xi + b_2\right] \tag{5}$$

where the following new parameters $\beta_i{}^{*}$ have been defined:

$$\beta_i{}^{*} = \frac{\beta_i}{1 - \beta_i} - \frac{\beta_{i-1}}{1 - \beta_{i-1}} \tag{6}$$

Integration of Eq. (5), in view of the integration rules of the distributions and after simple algebra, leads to the following explicit expressions for the transversal deflection function $u(\xi)$:

$$u(\xi) = c_1 + c_2\xi + c_3\left[\xi^2 + \sum_{j=1}^{n}\beta_i^*(\xi-\xi_i)^2 U(\xi-\xi_i)\right] + c_4\left[\xi^3 + \sum_{j=1}^{n}\beta_i^*(\xi^3 - 3\xi_i^2\xi + 2\xi_i^3)U(\xi-\xi_i)\right]$$
$$+ p^{[4]}(\xi) + \sum_{i=1}^{n}\beta_i^*\left[p^{[4]}(\xi) - p^{[4]}(\xi_i)\right]U(\xi-\xi_i) - \sum_{i=1}^{n}\beta_i^* p^{[3]}(\xi_i)(\xi-\xi_i)U(\xi-\xi_i) \tag{7}$$

where the integration constants have been re-defined as $c_3 = -b_2/2$, $c_4 = -b_1/6$, and the additional constant c_1, c_2 has been introduced.

Eq. (7) can be written is the following form useful for the subsequent algebraic manipulations.

$$u(\xi) = c_1 + c_2\xi + c_3 f_3(\xi) + c_4 f_4(\xi) + f_5(\xi) \tag{8}$$

in which, by comparison with Eq. (7), the definition of the functions $f_j(\xi)$, $j = 3, \ldots, 5$ is straightforward.

The closed form expression of the rotation function is straightforwardly related to the displacement first derivative: $\phi(\xi) = -u^I(\xi)$.

It has to be noted that the transversal displacement and the rotation functions, provided by Eq. (7) and its first derivative, respectively, are continuous functions despite the presence of the Heaviside generalised function appearing in Eq. (7). However, the curvature function, obtained as $\chi(\xi) = -u^{II}(\xi)$ by the second derivative of Eq. (7) presents discontinuities at cross sections ξ_i due to the flexural stiffness changes.

Eq. (7), where the integration constants c_1, c_2, c_3, c_4 are to be determined by imposing the relevant boundary conditions, represents the explicit solution of the multi-stepped Euler-Bernoulli beam subjected to any external transversal load. It is worth noting that continuous, discontinuous and singular (concentrated load) distribution laws can be considered in Eq. (7) by the terms related to the external load.

The exact solution of the stepped beam, expressed Eq. (7), is exploited in the next section for the definition of a non linear inelastic beam element whose shape function are related to the current beam state by considering a stepped beam whose stiffness distribution, for each step, is related to the corresponding inelastic deformation.

3. A novel inelastic beam finite element with distributed plasticity

In this section, by exploiting the closed form solution presented in Eq. (7), a novel displacement based beam element with distributed plasticity is formulated. Such an element is characterised by the capability of adapting its stiffness matrix by means of displacement shape functions enriched by generalised functions (distributions) including the effect of plastic deformation occurrences on transversal displacements. Accordingly, the proposed element will be addressed to as “Smart Displacement Based” (SDB) beam element to be distinguished by classical displacement based elements characterised by constant displacement shape functions independently on the plastic burden.

Within the non linear Newton–Raphson type iterative integration procedure, the displacement shape function updating is governed by the element state determined on the basis of integration of the cross-section plastic constitutive laws at the chosen Gauss points.

The adopted procedure represents the counterpart, in a displacement based approach, of those forced based procedures based on exact internal forces shape functions that are not affected by plastic occurrences [7–12]. Yet, the proposed procedure does not require additional inner iterations when it is adopted in a standard finite element (FE) displacement based (stiffness) code. Furthermore, the great advantage derived by operating in the displacement approach is that the deformed shape of each beam element is naturally derived by the displacement shape function without requiring any additional integration procedure as required by FB approaches [17].

Without lack of generality, with the aim of focussing on the capability of the generalised functions to capture the influence of plastic deformations on the in-plane bending behaviour only, the axial behaviour is not included in the model. However, some theoretical details regarding the out-of-plane bending are reported in the Appendix.

Finally, the shear deformability is also neglected since the so called *“flexural-shear interaction”* during the occurrence of the plastic deformations is still an open non trivial issue deserving an ad hoc study as also summarised in [46,47] and the references therein reported.

A great computational advantage of the proposed beam element is that no sub-element discretisation is required when abrupt changes of curvature occur between successive plastic beam segments. The number of degrees of freedom required during the non linear analysis remains unaltered with respect to the initial discretisation. The displacement field along the span of the beam element is that consistent with the model adopted for the plastic deformation distribution and is also able to account for the presence of any external load distribution.

3.1. Definition of the beam element

Since only the in-plane bending behaviour is considered, the new beam element is here defined in the x, z plane as shown in Fig. 2. The beam element connects joints i and j and the nodal displacements given by the transversal

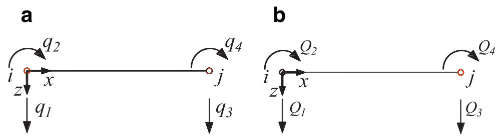

Fig. 2. The plane beam element: (a) nodal displacements, (b) nodal forces.

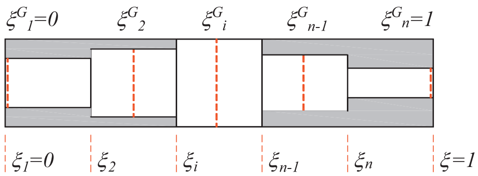

Fig. 3. The beam element subdivision into segment with reduced bending stiffness. (For interpretation of the references to colour in this figure legend, the reader is referred to the web version of this article.)

displacements and rotations at nodes i and j, as in Fig. 2a are collected in the vector $\mathbf{q}_e = \{q_1, q_2, q_3, q_4\}^T$. Furthermore, nodal forces provided by shear forces and bending moments at nodes i and j, as in Fig. 2b, are collected in the vector $\mathbf{Q}_e = \{Q_1, Q_2, Q_3, Q_4\}^T$.

3.2. The adopted displacement shape functions

The shape functions, adopted by classical formulations for the discretisation of the beam element displacement field, are based on the adoption of Hermite polynomials which, however, are not able to capture the curvature variations due to along axis plastic deformation occurrences. The latter circumstance results in the inadequacy of such shape functions to properly represent the displacement field in presence of flexural stiffness variations implied by plastic constitutive behaviour. On the contrary, the displacement based inelastic beam element proposed in this work, starting from the state of the homogeneous beam, aims at updating the displacement shape functions, according to the element state determination, depending on the local stiffness variations in the current element state.

To this aim the closed form solutions, enriched by the use of generalised functions, presented in the previous section for the multi-stepped beam, as in Eq. (7), are exploited to define suitable displacement shape functions for the beam element. The latter shape functions embed multiple stiffness variations with the great advantage of being dependent solely on the nodal degrees of freedom as for the homogeneous beam.

The numerical integration methods usually adopted to perform the element state determination are based on the Gauss procedure. The Gauss integration procedure provides approximations of integrals of regular functions over continuous domains by means of the values of the integrand at pre-established Gauss integration points, endowed with suitable weights. The chosen Gauss points represent control sections where the plastic constitutive laws are usually integrated according to a discrete incremental approach.

The present formulation regards the integration of functions containing distributions (generalised functions); the weight associated by the integration procedure to each Gauss point, assumed to be representative of the length of the beam segment with the reduced stiffness due to the plastic deformations, indicates the position of the generalised function steps occurring in Eq. (7) as specified in what follows.

In Fig. 3 an initially homogeneous beam with n Gauss points (*control sections*) is depicted. Precisely, in the current study, the Gauss–Lobatto integration scheme is used since the first and last integration points are always chosen coincident with the end sections. The weights and positions of the Gauss points are indicated as w_i and ξ_i^G, $i = 1, \ldots, n$, respectively.

According to the classical Newton–Raphson approach to solve non linear incremental problems in the context of holonomic plasticity in each time step, an incremental iterative solution procedure is followed in this work.

In the generic step of the incremental integration procedure in presence of plastic occurrences, the beam can be considered as subdivided into n segments of length w_i (length of the integration point) each characterised by a reduced bending stiffness $EI_i = EI(\xi_i^G)$ evaluated at the relevant Gauss point.

The position ξ_i^G of the integration points and the length of the reduces stiffness segment w_i, according to the Gauss–Lobatto integration procedure, imply abrupt changes of flexural stiffness with discontinuities in the curvature functions at abscissas $\xi_i = \sum_{j=1}^{i-1} w_j, \quad i = 1, 2, \ldots, n.$

The abscissas of the flexural stiffness discontinuity occurrences are collected in the vector $\boldsymbol{\xi}^{\mathbf{EI}} = \{\xi_1, \xi_2, \ldots, \xi_i, \ldots, \xi_n\}^T = \{0, w_1, (w_1 + w_2), \ldots, (w_1 + w_2 + \ldots + w_{n-1})\}^T$. On the other hand, the discontinuity parameters β_i and β_i^* are collected in the vectors $\boldsymbol{\beta} = \{\beta_1, \beta_2, \ldots, \beta_n\}^T$ and $\boldsymbol{\beta}^* = \{\beta_1^*, \beta_2^*, \ldots, \beta_n^*\}^T$, respectively.

The proposed SDB beam element is characterised by the parameters collected in the vectors $\boldsymbol{\xi}^{\mathbf{EI}}$ (positions of the flexural stiffness changes) and $\boldsymbol{\beta}^*$ (intensity of the flexural stiffness changes) required by Eqs. (7) and (8) for the beam with n flexural stiffness changes.

The shape functions of the transversal displacement $u(\xi)$ for the proposed beam element are determined by imposing the following nodal displacements and rotations:

$$u(0) = q_1; \quad \varphi(0) = -u^I(0) = -q_2; \quad u(1) = q_3; \quad \varphi(1) = -u^I(1) = -q_4 \tag{9}$$

Imposition of the boundary conditions in Eq. (9) onto the closed form expression proposed in Eq. (7), and its first derivative, leads to the expressions of the beam axis transversal deflection in terms of nodal displacements and the external load function as follows:

$$\begin{aligned} u(\xi;\boldsymbol{\xi}^{\mathbf{EI}},\boldsymbol{\beta}^*) &= \left[N_1(\xi;\boldsymbol{\xi}^{\mathbf{EI}},\boldsymbol{\beta}^*)N_2(\xi;\boldsymbol{\xi}^{\mathbf{EI}},\boldsymbol{\beta}^*)N_3(\xi;\boldsymbol{\xi}^{\mathbf{EI}},\boldsymbol{\beta}^*)N_4(\xi;\boldsymbol{\xi}^{\mathbf{EI}},\boldsymbol{\beta}^*)\right]\begin{bmatrix} q_1 \\ q_2 \\ q_3 \\ q_4 \end{bmatrix} + u_p\left(\xi;\boldsymbol{\xi}^{\mathbf{EI}},\boldsymbol{\beta}^*\right) \\ &= \mathbf{N}(\xi;\boldsymbol{\xi}^{\mathbf{EI}},\boldsymbol{\beta}^*)\cdot\mathbf{q}_e + u_p(\xi;\boldsymbol{\xi}^{\mathbf{EI}},\boldsymbol{\beta}^*) \end{aligned} \tag{10}$$

where $N_j(\xi;\ \boldsymbol{\xi}^{\mathbf{EI}},\ \boldsymbol{\beta}^*)$, $j = 1, \ldots, 4$, are the first four displacement shape functions, collected in the row vector $\mathbf{N}(\xi;\ \boldsymbol{\xi}^{\mathbf{EI}},\ \boldsymbol{\beta}^*)$, dependent on the abscissas and intensity of the flexural stiffness discontinuities in the vectors $\boldsymbol{\xi}^{\mathbf{EI}}$, $\boldsymbol{\beta}^*$, respectively, and the nodal displacements are collected in the vector $\mathbf{q}_e = [q_1 q_2 q_3 q_4]^T$. It is worth to notice that the last term in Eq. (10) $u_p(\xi;\boldsymbol{\xi}^{\mathbf{EI}},\boldsymbol{\beta}^*)$, dependent on the vectors $\boldsymbol{\xi}^{\mathbf{EI}}$, $\boldsymbol{\beta}^*$, provides the contribution of the external load $p(\xi)$ to the transversal displacement in addition to the displacement shape functions.

It has to be noted that the functions $N_j(\xi;\ \boldsymbol{\xi}^{\mathbf{EI}},\ \boldsymbol{\beta}^*)$, $j = 1, \ldots, 4$ and $u_p(\xi;\boldsymbol{\xi}^{\mathbf{EI}},\boldsymbol{\beta}^*)$ allow the reconstruction of the element deformed configuration once the nodal displacements are evaluated.

The explicit expressions of the shape functions $N_j(\xi;\ \boldsymbol{\xi}^{\mathbf{EI}},\ \boldsymbol{\beta}^*)$, $j = 1, \ldots, 4$ of the transversal displacement $u(\xi)$ of the beam axis in view of the compact Eq. (8) can be written as follows:

$$N_j(\xi;\boldsymbol{\xi}^{\mathbf{EI}},\boldsymbol{\beta}^*) = {}^jC_1 + {}^jC_2\xi + {}^jC_3 f_3(\xi) + {}^jC_4 f_4(\xi), \quad j = 1,\ldots,4 \tag{11}$$

where

$$\begin{aligned} &{}^1C_1 = 1;\ {}^1C_2 = 0;\ {}^1C_3 = -\frac{f_4{}^I(1)}{w};\ {}^1C_4 = \frac{f_3{}^I(1)}{w}; \\ &{}^2C_1 = 0;\ {}^2C_2 = 1;\ {}^2C_3 = \frac{-f_4{}^I(1) + f_4(1)f_2{}^I(1)}{w};\ {}^2C_4 = \frac{-f_3(1) + f_3{}^I(1)}{w}; \\ &{}^3C_1 = 0;\ {}^3C_2 = 0;\ C_3^3 = \frac{f'_4(1)}{w};\ {}^3C_4 = -\frac{f'_3(1)}{w}; \\ &{}^4C_1 = 0;\ {}^4C_2 = 0;\ {}^4C_3 = -\frac{f_4(1)}{w};\ {}^4C_4 = \frac{f_3(1)}{w}; \end{aligned} \tag{12}$$

while the term related to the contribution of the external load is given as follows:

$$u_p\left(\xi;\boldsymbol{\xi}^{\mathbf{EI}},\boldsymbol{\beta}^*\right) = \frac{f_4(1)f_5{}^I(1) - f_5(1)f_4{}^I(1)}{w} f_3(\xi) + \frac{f_5(1)f_3{}^I(1) - f_3(1)f_5{}^I(1)}{w} f_4(\xi) + f_5(\xi) \tag{13}$$

and

$$w = f_3(1)f_4{}^I(1) - f_4(1)f_3{}^I(1) \tag{14}$$

3.3. The element curvature and bending moment distribution

The curvature $\chi(\xi;\ \boldsymbol{\xi}^{\mathbf{EI}},\ \boldsymbol{\beta}^*)$ of the proposed plane beam element can be expressed in terms of nodal displacements and distributed external forces as follows:

$$\chi(\xi;\boldsymbol{\xi}^{\mathbf{EI}},\boldsymbol{\beta}^*) = \mathbf{B}(\xi;\boldsymbol{\xi}^{\mathbf{EI}},\boldsymbol{\beta}^*)\cdot\mathbf{q}_e - u_p^{II}\left(\xi;\boldsymbol{\xi}^{\mathbf{EI}},\boldsymbol{\beta}^*\right) \tag{15}$$

where $\mathbf{B}(\xi;\ \boldsymbol{\xi}^{\mathbf{EI}},\ \boldsymbol{\beta}^*)$, are defined as follows:

$$\mathbf{B}(\xi;\boldsymbol{\xi}^{\mathbf{EI}},\boldsymbol{\beta}^*) = \left[-N_1^{II}(\xi;\boldsymbol{\xi}^{\mathbf{EI}},\boldsymbol{\beta}^*) - N_2^{II}(\xi;\boldsymbol{\xi}^{\mathbf{EI}},\boldsymbol{\beta}^*) - N_3^{II}(\xi;\boldsymbol{\xi}^{\mathbf{EI}},\boldsymbol{\beta}^*) - N_4^{II}(\xi;\boldsymbol{\xi}^{\mathbf{EI}},\boldsymbol{\beta}^*)\right] \tag{16}$$

is a row vector the matrix collecting the curvature shape functions obtained as second derivatives of the transversal displacement shape functions containing the effect of the discontinuities. The function $u_p^{II}(\xi;\boldsymbol{\xi}^{\mathbf{EI}},\boldsymbol{\beta}^*)$ appearing in Eq. (15), also dependent on the state of the beam element, contains the contribution to the curvature function of the external distributed load $p(\xi)$.

In the presented plane beam element the normalised bending moment $M_z(\xi)$ is related to the curvature by means of the following relationship:

$$M(\xi;\boldsymbol{\xi}^{\mathbf{EI}},\boldsymbol{\beta}^*) = k(\xi;\boldsymbol{\xi}^{\mathbf{EI}},\boldsymbol{\beta})\ \chi(\xi;\boldsymbol{\xi}^{\mathbf{EI}},\boldsymbol{\beta}^*) \tag{17}$$

where $k(\xi;\boldsymbol{\xi}^{\mathbf{EI}},\boldsymbol{\beta}) = 1 - \sum_{i=1}^{n}(\beta_i - \beta_{i-1})U(\xi - \xi_i)$, according to Eq. (3), is the normalised cross-section flexural stiffness dependent on the β_i discontinuity parameters collected in the vector $\boldsymbol{\beta}$ and the position ξ_i of their occurrences.

In Eq. (17) the dependence of the flexural stiffness on the extension and intensity of the plastic zones through the non dimensional parameters ξ_i, β_i, according to the model proposed in Eq. (3), is indicated explicitly. The non linear variation of the flexural stiffness, as plastic deformations occur, will be explicit formulated by updating the vector $\boldsymbol{\beta}$, in the relevant beam segments identified by the vector $\boldsymbol{\xi}^{\mathbf{EI}}$, according to the sectional incremental constitutive law formulated in the next section.

3.4. The element stiffness matrix

The relationship between the normalised force and displacement element nodal vectors $\mathbf{Q}_e$ and q_e, respectively, can be inferred by the application of the principle of virtual work involving the curvature function $\chi(\xi)$ and the bending moment $M(\xi)$ as follows:

$$\mathbf{Q}_e^T\cdot\delta\mathbf{q}_e=\int_0^1 M(\xi;\boldsymbol{\xi}^{\mathbf{EI}},\boldsymbol{\beta}^*)\delta\chi(\xi;\boldsymbol{\xi}^{\mathbf{EI}},\boldsymbol{\beta}^*)\,d\xi\qquad\forall\delta\mathbf{q}_e,\delta\chi(\xi;\boldsymbol{\xi}^{\mathbf{EI}},\boldsymbol{\beta}^*)\tag{18}$$

where δ indicates virtual quantities. Substitution of the relation expressed by Eq. (17) into Eq. (18) leads to:

$$\mathbf{Q}_e^T\cdot\delta\mathbf{q}_e=\int_0^1 \chi(\xi;\boldsymbol{\xi}^{\mathbf{EI}},\boldsymbol{\beta}^*)\;k(\xi;\boldsymbol{\xi}^{\mathbf{EI}},\boldsymbol{\beta})\;\delta\chi(\xi;\boldsymbol{\xi}^{\mathbf{EI}},\boldsymbol{\beta}^*)\,d\xi\tag{19}$$

Further substitution of Eq. (15), purged of the external load contribution $u_p^{II}(\xi;\boldsymbol{\xi}^{\mathbf{EI}},\boldsymbol{\beta}^*)$, accounting for the proposed deformation shape functions of the multi-stepped beam, into Eq. (19) provides the following relationship:

$$\mathbf{Q}_e^T\cdot\delta\mathbf{q}_e=\mathbf{q}_e^T\cdot\int_0^1\mathbf{B}^{\mathbf{T}}(\xi;\boldsymbol{\xi}^{\mathbf{EI}},\boldsymbol{\beta}^*)k(\xi;\boldsymbol{\xi}^{\mathbf{EI}},\boldsymbol{\beta})\mathbf{B}(\xi;\boldsymbol{\xi}^{\mathbf{EI}},\boldsymbol{\beta}^*)\,d\xi\cdot\delta\mathbf{q}_e\tag{20}$$

Eq. (20) implies the following relationship between the force and displacement element nodal vectors $\mathbf{Q}_e$ and q_e:

$$\mathbf{Q}_e=\mathbf{K_e}(\boldsymbol{\xi}^{\mathbf{EI}},\boldsymbol{\beta},\boldsymbol{\beta}^*)\cdot\mathbf{q}_e\tag{21}$$

where $\mathbf{K_e}(\boldsymbol{\xi}^{\mathbf{EI}},\boldsymbol{\beta},\boldsymbol{\beta}^*)$ is the element stiffness matrix, dependent on the current state of the element by means of the plastic intensity parameter vectors $\boldsymbol{\beta},\boldsymbol{\beta}^*$ and the plastic segment extension vector $\boldsymbol{\xi}^{\mathbf{EI}}$, defined as follows:

$$\mathbf{K_e}(\boldsymbol{\xi}^{\mathbf{EI}},\boldsymbol{\beta},\boldsymbol{\beta}^*)=\int_0^1\mathbf{B}^{\mathbf{T}}(\xi;\boldsymbol{\xi}^{\mathbf{EI}},\boldsymbol{\beta}^*)k(\xi;\boldsymbol{\xi}^{\mathbf{EI}},\boldsymbol{\beta})\mathbf{B}(\xi;\boldsymbol{\xi}^{\mathbf{EI}},\boldsymbol{\beta}^*)\,d\xi\tag{22}$$

The expression reported in Eq. (22) shows clearly how the element stiffness matrix $\mathbf{K_e}$, differently from the classical displacement based approach commonly adopted in the literature, depends on the variation of the shape functions which are updated in accordance to the parameter vector $\boldsymbol{\beta}^*$.

According to the Gauss integration scheme the element stiffness matrix in Eq. (22) can be evaluated as follows:

$$\mathbf{K_e}(\boldsymbol{\xi}^{\mathbf{EI}},\boldsymbol{\beta},\boldsymbol{\beta}^*)\approx\sum_{r=1}^{N}\mathbf{B}^{\mathbf{T}}(\xi_r^G;\boldsymbol{\xi}^{\mathbf{EI}},\boldsymbol{\beta}^*)k(\xi_r^G;\boldsymbol{\xi}^{\mathbf{EI}},\boldsymbol{\beta})\mathbf{B}(\xi_r^G;\boldsymbol{\xi}^{\mathbf{EI}},\boldsymbol{\beta}^*)\,w_r\tag{23}$$

In Eq. (23) N is the number of Gauss points adopted in the integration scheme. In the numerical applications conducted in the present study different integrations have been performed by considering N varying up to 10 Gauss points.

It is worth noting that the curvature shape functions involved in the matrix $\mathbf{B}(\xi;\ \boldsymbol{\xi}^{\mathbf{EI}},\ \boldsymbol{\beta}^*)$, since obtained by the second derivative of the displacement shape functions reported in Eq. (10), are discontinuous functions at cross sections $\xi_i=\sum_{j=1}^{i-1}w_r,\quad i=1,2,\dots,n$ where the bending stiffness undergoes abrupt changes in the considered model. The extended form of the element stiffness matrix $\mathbf{K_e}(\boldsymbol{\xi}^{\mathbf{EI}},\boldsymbol{\beta},\boldsymbol{\beta}^*)$ provided by Eq. (23), in view of Eqs. (16), is reported as follows::

$$\mathbf{K_e}(\boldsymbol{\xi}^{\mathbf{EI}},\boldsymbol{\beta}^*)=\sum_{r=1}^{N}\begin{bmatrix}k(\xi_r^G)N_1^{II^2}(\xi_r^G) & k(\xi_r^G)N_1^{II}(\xi_r^G)N_{y2}^{II}(\xi_r^G) & k(\xi_r^G)N_1^{II}(\xi_r^G)N_{z3}^{II}(\xi_r^G) & k(\xi_r^G)N_1^{II}(\xi_r^G)N_4^{II}(\xi_r^G)\\ & k(\xi_r^G)N_2^{II^2}(\xi_r^G) & k(\xi_r^G)N_2^{II}(\xi_r^G)N_3^{II}(\xi_r^G) & k(\xi_r^G)N_2^{II}(\xi_r^G)N_4^{II}(\xi_r^G)\\ & & k(\xi_r^G)N_3^{II^2}(\xi_r^G) & k(\xi_r^G)N_3^{II}(\xi_r^G)N_4^{II}(\xi_r^G)\\ sym & & & k(\xi_r^G)N_4^{II^2}(\xi_r^G)\end{bmatrix}w_r\tag{24}$$

The terms in Eq. (24) deserving attention, with respect to the standard stiffness matrix formulation, are the curvature shape functions $N_j^{II}(\xi_r^G;\boldsymbol{\xi}^{\mathbf{EI}},\boldsymbol{\beta}^*),\ j=1,\dots,4$ evaluated at the Gauss points ξ_r^G, to be updated during the iterative procedure.

3.5. The nodal resisting forces and the nodal forces equivalent to the external load

Besides the element constitutive relation in terms of nodal force and displacement quantities expressed by Eq. (21), the normalised element nodal resisting forces Q_e to be replaced in the structural global equilibrium equations can be determined, again, by making use of the principle of virtual work as formulated in Eq. (18). However, in this case, substitution of Eq. (15) into Eq. (18) leads to:

$$\mathbf{Q}_e^T\cdot\delta\mathbf{q}_e=\int_0^1 M(\xi;\boldsymbol{\xi}^{\mathbf{EI}},\boldsymbol{\beta}^*)\mathbf{B}(\xi;\boldsymbol{\xi}^{\mathbf{EI}},\boldsymbol{\beta}^*)\,d\xi\ \cdot\delta\mathbf{q}_e\tag{25}$$

Eq. (25) implies the following definition for the element nodal resisting forces in terms of bending moment distribution $M(\xi;\ \boldsymbol{\xi}^{\mathbf{EI}}, \boldsymbol{\beta}^*)$:

$$\mathbf{Q}_e(\boldsymbol{\xi}^{\mathbf{EI}}, \boldsymbol{\beta}^*) = \int_0^1 \mathbf{B}^{\mathbf{T}}(\xi; \boldsymbol{\xi}^{\mathbf{EI}}, \boldsymbol{\beta}^*) M(\xi; \boldsymbol{\xi}^{\mathbf{EI}}, \boldsymbol{\beta}^*)\, d\xi \tag{26}$$

As considered for the element stiffness matrix, the expression reported in Eq. (26) shows that the element nodal resisting forces Q_e, differently from the classical displacement based approach commonly adopted in the literature, depends on the variation of the shape functions which are updated in accordance to the parameter vector $\boldsymbol{\beta}^*$ and the related discontinuity position vector $\boldsymbol{\xi}^{\mathbf{EI}}$.

The element nodal resisting forces Q_e, provided by Eq. (26), can be numerically evaluated according to the Gauss integration scheme as follows:

$$\mathbf{Q}_e(\boldsymbol{\xi}^{\mathbf{EI}}, \boldsymbol{\beta}^*) \approx \sum_{r=1}^{N} \mathbf{B}^{\mathbf{T}}(\xi_r^G; \boldsymbol{\xi}^{\mathbf{EI}}, \boldsymbol{\beta}^*) M(\xi_r^G; \boldsymbol{\xi}^{\mathbf{EI}}, \boldsymbol{\beta}^*)\, w_r \tag{27}$$

Again, the number of Gauss points N appearing in Eq. (27) have been considered, in the numerical applications reported in Section 5, variable from a minimum of 3 up to 10 Gauss points.

On the other hand, the nodal forces equivalent to the along axis external forces, to be balanced by the internal forces determined by means of Eq. (27), are given as:

$$\mathbf{P}_e(\boldsymbol{\xi}^{\mathbf{EI}}, \boldsymbol{\beta}^*) = \int_0^1 \mathbf{N}^{\mathbf{T}}(\xi; \boldsymbol{\xi}^{\mathbf{EI}}, \boldsymbol{\beta}^*) p(\xi)\, d\xi \tag{28}$$

The element nodal external forces P_e, provided by Eq. (28), can be numerically evaluated according to the Gauss integration scheme as follows:

$$\mathbf{P}_e(\boldsymbol{\xi}^{\mathbf{EI}}, \boldsymbol{\beta}^*) \approx \sum_{r=1}^{N} \mathbf{N}^{\mathbf{T}}(\xi_r^G; \boldsymbol{\xi}^{\mathbf{EI}}, \boldsymbol{\beta}^*) p(\xi_r^G)\, w_r \tag{29}$$

4. The sectional constitutive law and the exact solution for straight beams

In this section the constitutive law, adopted to perform the non linear plastic analysis, of beam elements, is specified. In particular, since the aim of the work is testing the performance of the shape functions proposed in the previous section against exact solutions, an elastic- perfectly plastic behaviour of the material (i.e. no plastic hardening/softening is allowed both in tension and compression) is assumed. However, it has to be pointed out that introduction of a linear or non linear post elastic material behaviour can also be treated by suitable integration of the constitutive law at Gauss point level by means of known procedures available in the literature.

According to a perfectly plastic behaviour, a cross section subject to bending undergoes a development of plastic deformations, dependent on the stress distribution across the height, following the material fibres that progressively exceed the yield stress σ_o. The latter phenomenon determines a non linear inelastic bending moment-curvature relationship ruled by the geometry of the cross-section.

For the case of rectangular cross section, defined by width b and height $2h$, and material with no hardening/softening, the relationship between bending moment $M(\xi)$ and curvature $\chi(\xi)$ can be written, by using dimensional quantities, as follows [30]:

$$\chi = \begin{cases} \frac{3}{2}\frac{M}{Ebh^3} & \text{if} \quad |M| \le M_e \\ -\frac{K}{\sqrt{M_p - |M|}} & \text{if} \quad |M| > M_e \end{cases} \tag{30}$$

where $M_e = \frac{2}{3}bh^2\sigma_o$ and $M_p = bh^2\sigma_o$ are the limit elastic moment and the fully plastic moment, respectively, being $|M| = M_e$ the condition for initiation of plastic deformation starting at the curvature value $\chi_e = \frac{\sigma_o}{Eh}$. Furthermore, the constant K in Eq. (30) is defined as $K = sign[-M]\sqrt{\frac{b\sigma_o^3}{3E^2}}$. The bending moment-curvature relationship in Eq. (30) is plotted in Fig. 4.

Once the bending moment-curvature relationship has been set, Eq. (30) itself, in view of the relationship $\chi = -\frac{d^2u}{dx^2}$, can be considered as a second order non linear differential equation to be integrated over the beam domain $\Omega = [0, L]$ to be partitioned into n_e elastic subdomains $\Omega_e^{(i)}$, $i = 1, \ldots, n_e$, (where $|M| \le M_e$) and n_p plastic sub-domains $\Omega_p^{(j)}$, $j = 1, \ldots, n_p$, (where $|M| > M_e$) as follows:

$$\frac{d^2u(x)}{dx^2} = \begin{cases} -\frac{3}{2}\frac{M(x)}{Ebh^3} & \text{in} \quad \Omega_e^{(i)},\ i = 1, \ldots, n_e \\ \frac{K}{\sqrt{M_p - |M(x)|}} & \text{in} \quad \Omega_p^{(j)},\ i = 1, \ldots, n_p \end{cases} \tag{31}$$

Integration of Eq. (31) is particularly convenient for statically determinate beams since the bending moment distribution is dependent only on the external loads and consequently the domain subdivision into elastic and plastic sub-domains can be a priori inferred and are not influenced by the presence of plastic strains.

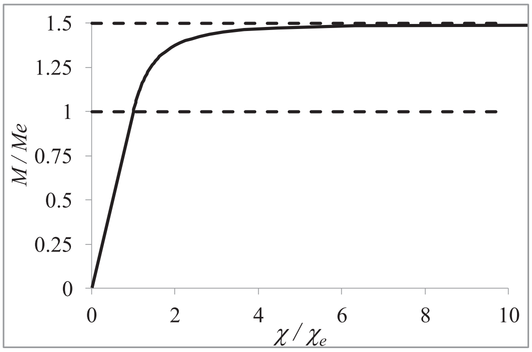

Fig. 4. The bending moment-curvature relationship in Eq. (30) for a rectangular cross-section with elastic, perfectly plastic material.

Precisely, the closed form solution of Eq. (31) in terms of displacement $u_y(x)$ proposed in [30] is obtained by the sum of the homogeneous $u_y^H(x)$ and a particular $u_y^P(x)$ solution as follows:

$$u(x) = u^H(x) + u^P(x) \tag{32}$$

where the homogeneous solution is given as $u^H(x) = C_1 x + C_2$, being C_1, C_2 integration constants. A particular solution for a second order polynomial form for the bending moment $M(x) = m_2 x^2 + m_1 x + m_o$, as in the most common load cases, is as follows in the elastic sub-domains $\Omega_e^{(i)}$, $i = 1, \ldots, n_e$:

$$u^P(x) = -\frac{x^2}{8Ebh^3}(m_2 x^2 + 2m_1 x + 6m_o) \tag{33}$$

while it takes the following forms in the plastic sub-domains $\Omega_p^{(i)}$, $i = 1, \ldots, n_p$ according to the degree n = 0, 1, 2 of the bending moment polynomial:

$$u^P(x) = \frac{K}{2\sqrt{M_p - |m_o|}} x^2 \quad \text{for} \quad n = 0$$

$$u^P(x) = \frac{4K}{3m_1^2}\sqrt{(M_p - |M(x)|)^3} \quad \text{for} \quad n = 1$$

$$u^P(x) = \begin{cases} \frac{K}{2\sqrt{|m_2|^3}}\left[T(x)\arcsin\left(\frac{T(x)}{|D|}\right) + \sqrt{D^2 - T^2(x)}\right] & \text{if} \quad \mathrm{sign}[M(x)]m_2 > 0 \\ \frac{K}{2\sqrt{|m_2|^3}}\left[T(x)\mathrm{arsh}\left(\frac{T(x)}{|D|}\right) - \sqrt{D^2 + T^2(x)}\right] & \text{if} \quad \mathrm{sign}[M(x)]m_2 < 0 \end{cases} \quad \text{for} \quad n = 2 \tag{34}$$

where $T(x)$ is the shear force distribution and D is the discriminant of the second order equation $M_p - |M| = 0$.

The non linear constitutive law for a rectangular cross section reported in Eq. (30) will be adopted in the following applications.

The closed form solution in terms of displacement function reported in Eqs. (32)–(34) is adopted as a benchmark solution to test the performance of the proposed SDB beam element for a specific case of straight beam already treated in the literature. In other cases the proposed element is tested against the classical DB finite element approach, a FB approach and a mixed approach.

5. Applications

5.1. Cantilever beam

The case of cantilever beam with a concentrated tip load with length $L = 4$ m and rectangular cross section with width $b = 30$ cm and height $2h = 40$ cm, is considered first. The material is characterised by Young modulus $E = 210000$ MPa and yield stress $\sigma_o = 300$ MPa and the cross section bending moment-curvature constitutive law is given by Eq. (30) with $M_e = 2400$ kNm, $M_p = 3600$ kNm and $\chi_e = 7, 14286 \cdot 10^{-5}$ cm^{-1}.

On the account of the above considered material and geometric data, the ultimate load of the cantilever beam is $F_p = 900$ kN. The following numerical applications are based on different approaches and have been executed by means of the Newton–Raphson iterative algorithm by considering different numbers of FEs for the along axis discretisation.

Fig. 5 shows the tip load value versus the vertical displacement of the end cross section. The analyses have been performed by means of the proposed SDB FE by making use of displacement shape function updating during the plastic deformation occurrences and by means of the classical DB FE with constant shape functions. In both cases, five integration points have been considered in each non linear finite element.

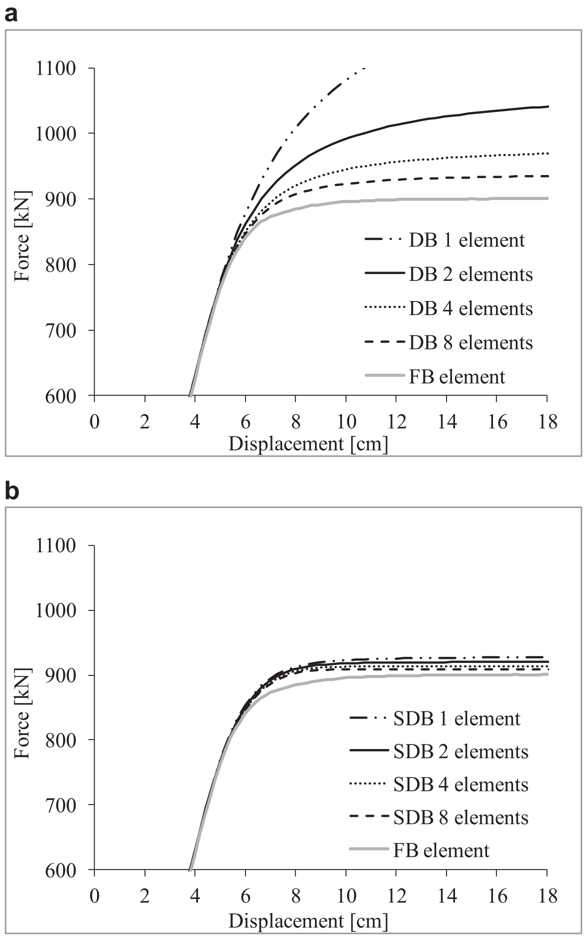

Fig. 5. Tip load-vertical displacement curve of the cantilever beam: (a) classical DB versus FB approach; (b) proposed SDB versus FB approach.

Table. 1
Ultimate load error of the SDB and DB approaches for different FE discretisation.

	Number of Elements	1	2	4	8
SDB	F [kN]	927,47	920,18	913,83	909,07
	Error [%]	3,05	2,24	1,54	1,01
DB	F [kN]	1195,72	1040,92	969,15	934,82
	Error [%]	32,86	15,66	7,68	3,87

In particular, in Fig. 5a and b the force-displacement curves for an increasing number of classical DB FEs and by means of the proposed SDB FE, respectively, are plotted and compared with the FB approach obtained with the SeismoStruct software [46].

Analysis of Fig. 5 reveals that updating the shape functions during the iterative integration procedure, according to expressions reported in Eqs. (11), (12) and the related expressions of the stiffness matrix and the nodal forces, results in a better performance of the displacement based approach (if generalised functions are employed) requiring a small number of elements for an accurate analysis.

The details of the errors of the DB and SDB approaches with respect to the theoretical ultimate load $F_p = 900$ kN are reported in Table. 1.

It has to be noted an error of about 3% if a single beam element with updating shape functions is adopted, compared to almost 33% error if the displacement shape functions are kept constant.

Furthermore, the performance of the proposed approach for different numbers of integration points has been tested. In Fig. 6a and b the tip load-vertical displacement curves for the DB and SDB approaches are reported for 3,5,10 integration points. It can be seen that the results are not sensitive to the number of integration points if the minimum number of 5 is adopted. The errors, in terms of ultimate load are reported in Table. 2.

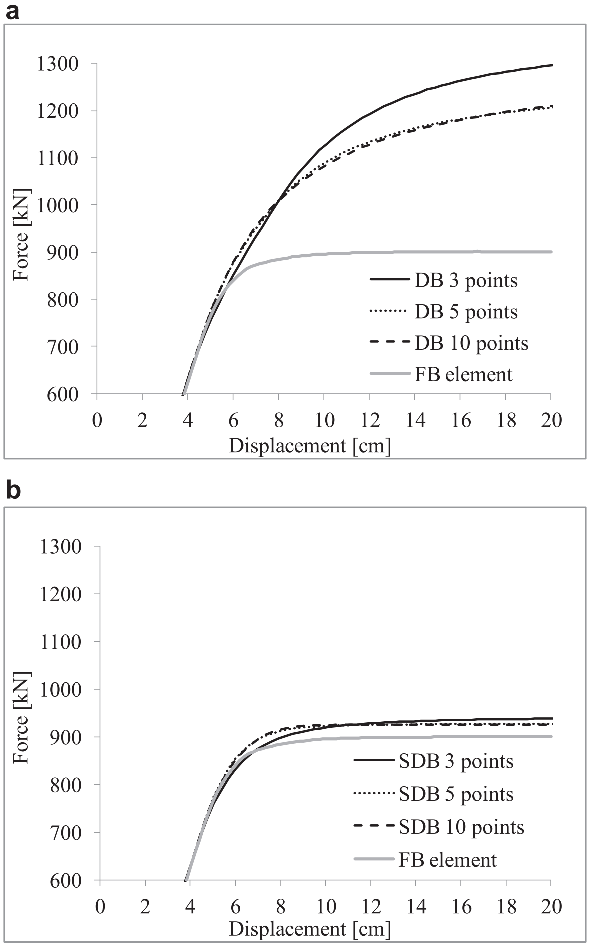

Fig. 6. Tip load-vertical displacement curve of the cantilever beam for different numbers of integration points: (a) classical DB versus FB approach; (b) proposed SDB versus FB approach.

Table. 2
Ultimate load error of the SDB and DB approaches for different number of integration points.

	Number of integration points	3	5	10
SDB	F [kN]	938,42	927,47	925,90
	Error [%]	4,27	3,05	2,88
DB	F [kN]	1296,80	1207,21	1211,39
	Error [%]	44,09	34,13	34,60

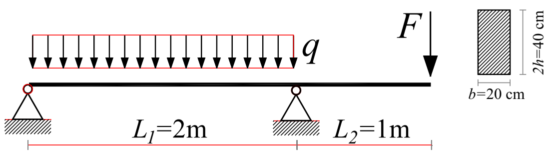

Fig. 7. A simply supported overhanging beam with a distributed and a concentrated load.

5.2. Simply supported overhanging beam

The simply supported overhanging beam reported in Fig. 7 with lengths $L_1 = 2$ m, $L_2 = 1$ m has been also studied with the purpose of testing the proposed SDB FE against the closed form solution, able to describe the diffusion of plasticity, proposed by Stock and Halilovic [30] according to the procedure summarized in Section 4. The beam has a rectangular cross

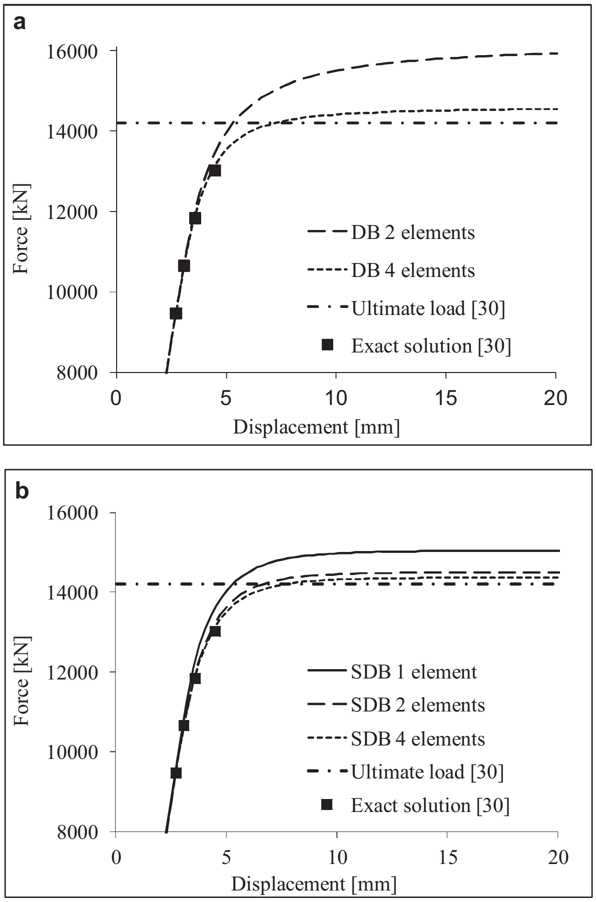

Fig. 8. Vertical load – vertical displacement (at the position of the maximum bending moment) curve of the simply supported overhanging beam in Fig. 7 for $\psi = 0.127$ with an increasing number of FEs: (a) DB FE; (b) SDB FE.

section with width $b = 20$ cm and height $2h = 40$ cm and the material properties, together with the non linear bending moment-curvature relationship, are those already adopted in the application of the Section 5.1.

The beam in Fig. 7 is subjected to a concentrated force F at its free end and a uniformly distributed load q between the supports. Stock and Halilovic [30] studied the diffusion of plasticity as the loading parameter λ (multiplying both external loads λF, λq, i.e. proportional loading is assumed) increases, for different values of the ratio $\psi = \frac{F}{qL_1}$ between the external loads governing the location of the maximum bending moment and position of the plastic yielding initiation.

In the applications the following two values of the external load ratio will be considered: *case 1)* $\psi = 0.127$, inducing plastic yielding between the two supports; *case 2)* $\psi = 0.225$ leading to yielding at the right support. The limit elastic moment is $M_e = 1600$ kNm, while the couples of ultimate load values, inferred by the value of the fully plastic moment $M_p = 2400$ kNm, are as follows: *case 1)*$F_p = 1600$ kN, $q_p = 63 kNcm$; *case 2)*$F_p = 2400$ kN, $q_p = 53.33$ *kNcm*.

In Fig. 8 the results of the incremental analysis in terms of total vertical load $V = F + qL_1$ versus the vertical displacement at the position of the maximum bending moment for *case 1*) (ultimate vertical load $V_p = 14200$ kN) are plotted. Precisely, Fig. 8a reports the curves for an increasing number of classical DB FE, while Fig. 8b the curves obtained through the proposed SDB FE and the results are compared with the exact incremental solution by Table. 1 of the paper [30].

Precisely, Fig. 8a and b are relative to *case 1)* (ultimate vertical load $V_p = 14200$ kN) and *case 2)* (ultimate vertical load $V_p = 13066$ kN), respectively.

Fig. 9 reports the results of the incremental analysis in terms of total vertical load $V = F + qL_1$ versus the vertical displacement of the free end *(case 2)* for an increasing number of the classical DB FE (Fig. 9a) and the proposed SDB FE (Fig. 9b) and compared with the exact incremental solution by Table. 1 of the paper [30].

On the other hand, in order to show how the proposed element improves the performance of classical shape functions, the errors of the SDB and the DB FE approaches in terms of ultimate load value, evaluated with respect to the exact solution, are reported for comparison purposes in Table. 3.

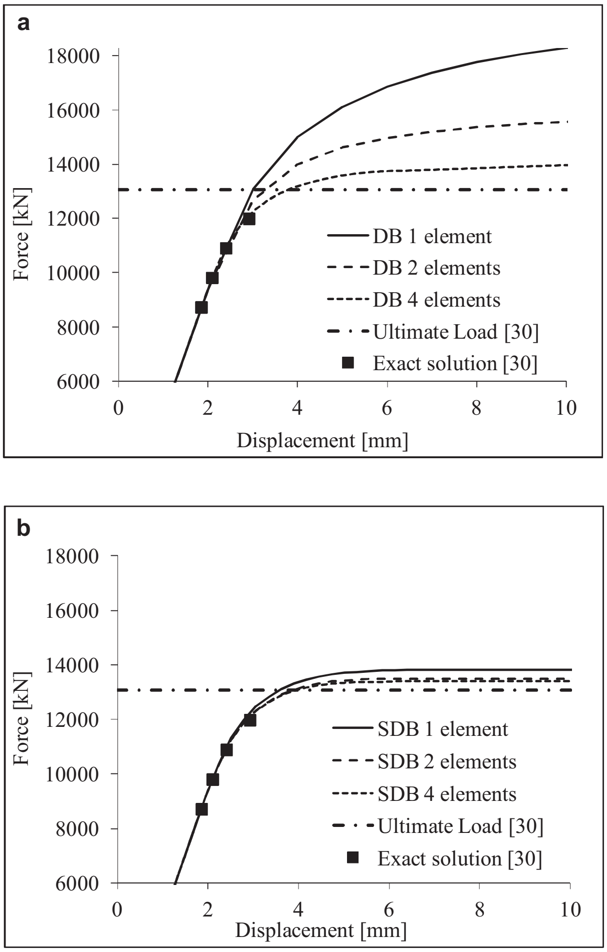

Fig. 9. Total Vertical load – vertical displacement (at the free end of the beam) curve of the simply supported overhanging beam in Fig. 7 for $\psi = 0.225$ with an increasing number of FEs: (a) DB FE model; (b) SDB FE model.

Table. 3
Ultimate load error of the SDB and DB approaches for different FE discretisation.

	$\psi = 0.127$		$\psi = 0.225$	
	Ultimate Load [kN]	error [%]	Ultimate Load [kN]	error [%]
Exact solution [30]	14196,79	–	13059,65	–
1 element SDB	15049,68	6,01	13847,82	6,04
1 element DB	–	–	19794,68	51,57
2 elements SDB	14498,27	2,12	13622,92	4,31
2 elements DB	16088,61	13,33	16061,61	22,99
4 elements SDB	14364,17	1,18	13394,31	2,56
4 elements DB	14601,78	2,85	14217,67	8,87

The deformed shape of the entire beam obtained by means of the proposed approach, provided by Eq. (10) is also plotted in Fig. 10 both for *case 1)* and *case 2)* and compared with the exact solution.

The diffusion of plasticity, captured by the segments of the beam subjected to stiffness reduction, is evidenced both for *case 1)* and *case 2)* in Fig. 11 as the number of SDB FE increases. Obviously, plastic deformation diffusion is more detailed as the number of FE, or alternatively the number of Gauss points, increases.

5.3. Simply supported beam with concentrated load in presence of hardening

The single span simply supported beam with a point load concentrated at the middle cross section reported in Fig. 12, studied in [23] by means of mixed FE formulation, has been also analysed by means of the proposed SDB FE for further comparison purposes.

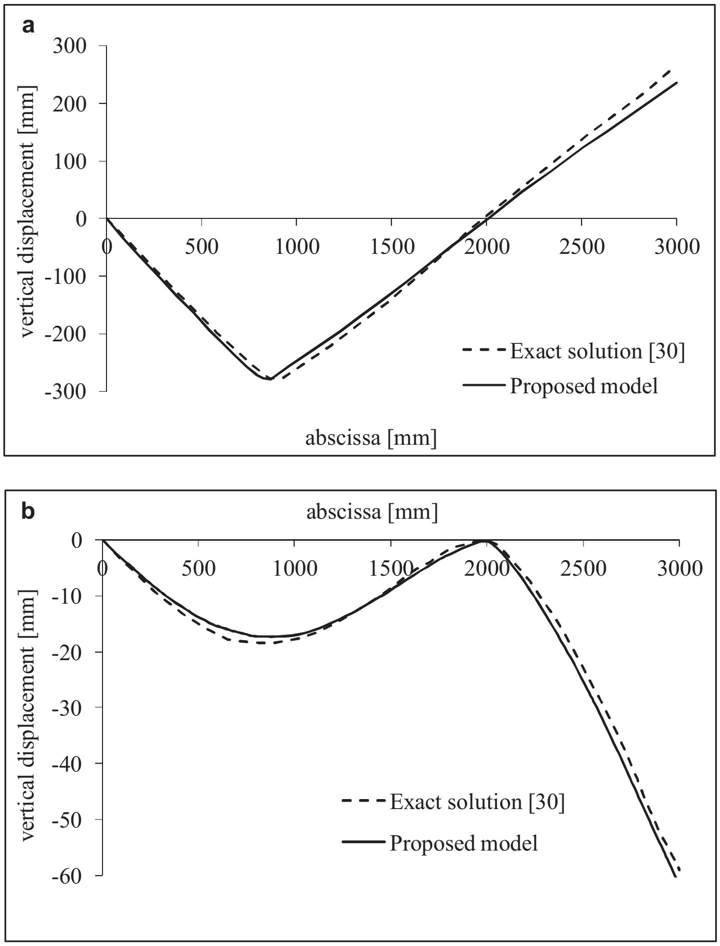

Fig. 10. Deformed shape of the beam in Fig. 7:(a) *case 1)* $\psi = 0.127$ yielding in the span; (b) *case 2)* $\psi = 0.225$ yielding in the overhanging portion.

The geometric and physical properties of the beam are as follows: beam length $L = 180$ cm, rectangular cross section with width $b = 10$ cm and height $2h = 10$ cm, Young modulus $E = 290.000$ MPa, yield stress $\sigma_0 = 500$ MPa and a 1% linear hardening with respect to the elastic modulus. The beam is modelled with two elements and five Gauss–Lobatto integration points are considered along each beam element. In the paper [23] the mixed FE formulation has been compared with the solution obtained by using a standard DB FE model with cubic Hermite polynomial shape functions by adopting two, four and eight elements for the discretisation of the entire beam. The latter comparison in terms of force-displacement relation, beam deformed shape and distribution of the bending moment and curvature along the beam length, showed the superiority of the mixed formulation with respect to the standard DB FE model. The contribution provided by the present work aims at improving the performance of the DB FE approach by introducing the adoption of generalised function in the displacement shape functions and considering their updating in the elastic-plastic analysis. For this reason the force-displacement curve at the middle cross section provided in [23], corresponding to the mixed model (MB), is here enriched with the results obtained with the traditional displacement FE model (DB) and the smart displacement model (SDB). The graph is reported in Fig. 12 and shows that the proposed approach, aiming at keeping unaltered the standard displacement approach although based on shape functions updating, provides results comparable to those provided by the mixed approach.

It can be concluded that the SDB FE approach improves drastically the poor performance of the standard displacement approach, the latter being the main reason that motivated alternative approaches accounting for force distribution modelling along the finite element. It has to be noted that the mixed formulation presented in [23] requires the choice of Gauss–Lobatto points also along the depth of the beam that is not required by the formulation here presented.

6. Conclusions

This work provided an improvement of the performance of the DB (stiffness matrix) finite element approach for the elastic-plastic analysis of beam-like and frame structures. Precisely, it has been shown that accurate results can be achieved by avoiding a discretisation of each structural member into several finite elements (mesh refinement) or by the introduc-

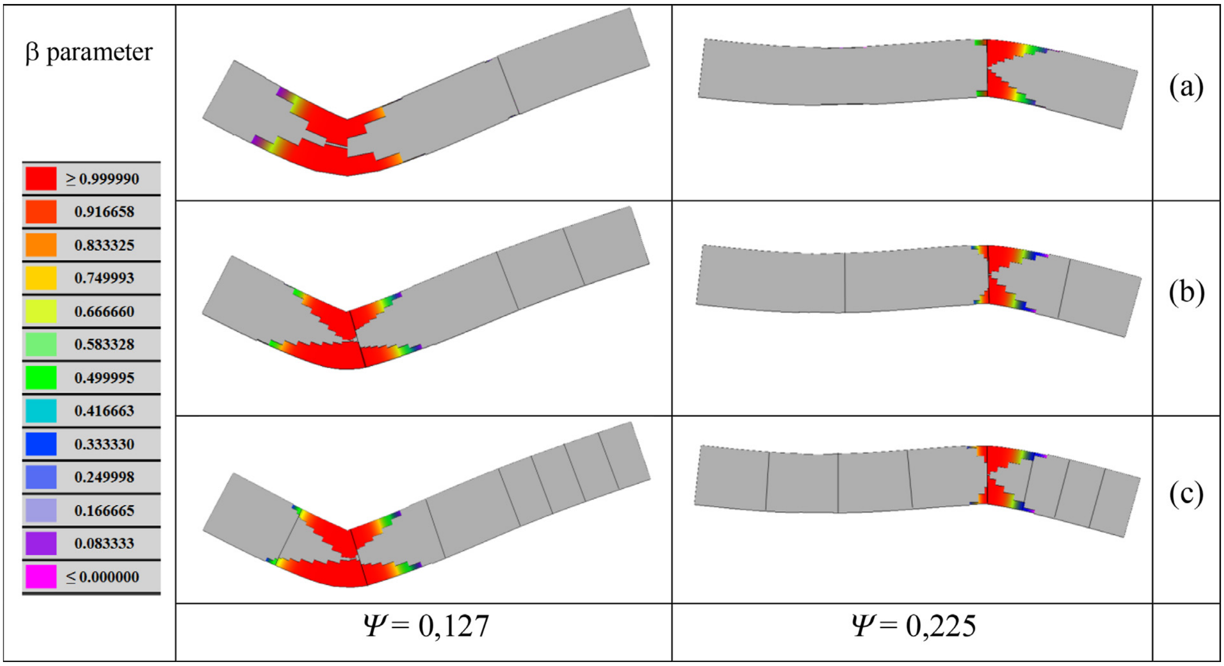

Fig. 11. Diffusion of plastic deformation in the beam of Fig. 7:(a) n.1 SDB FE; (b) n.2 SDB FEs; (c) n.4 SDB FEs.

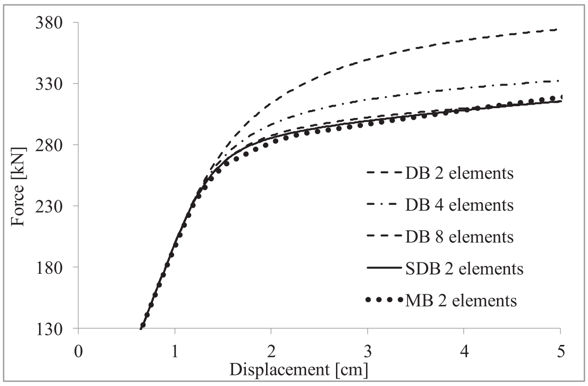

Fig. 12. Force – displacement (at middle cross section) curve of the simply supported beam studied in [23].

tion of higher order displacement shape functions. Hence, the increment of the number of degrees of freedom and the consequent reduction of the computational efficiency required by the classical DB approach for a better accuracy is avoided.

The strategy pursued in this study relies on the adoption of the explicit solution of stepped beams (i.e. beams with abrupt cross section variations) to model flexural stiffness reductions over portions of the beam due to the occurrence of plastic deformations. The latter solution has been formulated by means of the use of generalised functions (distributions) which allow to express the solution as a function of the end degrees of freedom only as in the uniform beam. The adopted analytical solution allows the construction of displacement shape functions to be updated according to the stiffness reduction caused by the post-yielding material behaviour. The above displacement shape function updating is built in the iterative procedure of the Newton–Raphson type and leads to enriched forms of the structural stiffness matrix, internal and external nodal forces with respect to the standard constant displacement shape function approach.

The proposed procedure has been tested both for beam-like and frame structures and, in particular, against the exact solution available in the literature for a simply supported overhanging beam. The latter solution has been adopted as a benchmark for the plasticity diffusion due to bending moment-curvature nonlinear curve inferred by a rectangular cross section with an elastic, perfectly plastic material.

The results of the proposed procedure, denoted in this work as SDB (Smart Displacement Based) approach, have led to a drastic improvement of the displacement based finite element discretisation, within the context of diffused plasticity models, competitive with both force based and mixed approaches.

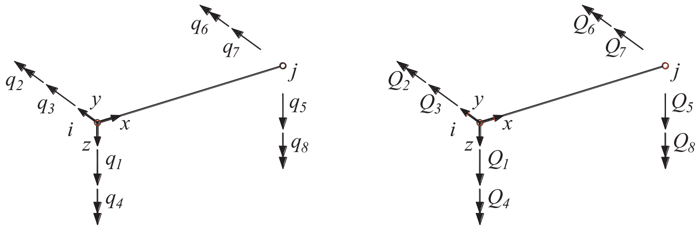

Fig. A1. The out-of-plane beam element: (a) nodal displacements, (b) nodal forces.

Appendix. The out-of-plane flexural SDB element

A brief description of some details regarding the generalisation of the proposed SDB beam element to the case of out-of-plane bending behaviour is reported in this appendix for the benefit of the interest reader.

In case of out-of-plane bending behaviour, the SDB beam element is here defined in the *x, y, z* Cartesian space as shown in Fig. A1. The nodal displacements given by the transversal displacements and rotations at nodes *i* and *j*, as in Fig. A1 are collected in the vector $\mathbf{q}_e = \{q_1, q_2, q_3, q_4, q_5, q_6, q_7, q_8\}^T$. Furthermore, nodal forces provided by shear forces and bending moments at nodes *i* and *j*, as in Fig. 2b, are collected in the vector $\mathbf{Q}_e = \{Q_1, Q_2, Q_3, Q_4, Q_5, Q_6, Q_7, Q_8\}^T$.

The distributional model for the flexural stiffness of a multi-stepped beam adopted in this work can be extended to the out-of-plane behaviour by considering the components of the normalised flexural stiffness, both for the *x, z* and *x, y* planes, as follows:

$$k_z(\xi;\boldsymbol{\xi}^{\mathbf{EI}},\hat{\boldsymbol{\beta}}_\mathbf{z}) = 1-\sum_{i=1}^{n}(\hat{\beta}_{z,i}-\hat{\beta}_{z,i-1})U(\xi-\xi_i)$$
$$k_y(\xi;\boldsymbol{\xi}^{\mathbf{EI}},\hat{\boldsymbol{\beta}}_\mathbf{y}) = 1-\sum_{i=1}^{n}(\hat{\beta}_{y,i}-\hat{\beta}_{y,i-1})U(\xi-\xi_i) \tag{A1}$$

In Eq. (A1), in order to take into account the out-of-plane influence of the discontinuity parameters, the new parameters (with the superimposed hat) $\hat{\beta}_{z,i} = \beta_{z,i}+\kappa_z\beta_{y,i}$ and $\hat{\beta}_{y,i} = \beta_{y,i}+\kappa_y\beta_{z,i}$ have been introduced. The two constants κ_z, κ_y, dependent on the geometric and physical cross section properties and representing the mutual influence of $\beta_{z,i}$ and $\beta_{y,\,i}$, are zero for the elastic state, being *y* and *z* principal inertia axes, and are to be updated during the plastic analysis, being related to the current state of the beam sections.

Furthermore, for convenience, in Eq. (A1) the vectors $\hat{\boldsymbol{\beta}}_\mathbf{z} = [\hat{\beta}_{z,1}\hat{\beta}_{z,2}\ldots\hat{\beta}_{z,n}]^T$ and $\hat{\boldsymbol{\beta}}_\mathbf{y} = [\hat{\beta}_{y,1}\hat{\beta}_{y,2}\ldots\hat{\beta}_{y,n}]^T$ have been introduced.

The closed form expression proposed in Eq. (7) for the in-plane behaviour is extended to the out-of-plane case by means of the following expressions for the transversal displacements $u_z(\xi)$ and $u_y(\xi)$:

$$u_z(\xi) = c_{z1}+c_{z2}\xi+c_{z3}f_{z3}(\xi)+c_{z4}f_{z4}(\xi)+f_{z5}(\xi)$$
$$u_y(\xi) = c_{y1}+c_{y2}\xi+c_{y3}f_{y3}(\xi)+c_{y4}f_{y4}(\xi)+f_{y5}(\xi) \tag{A2}$$

where

$$f_{z3}(\xi) = \xi^2+\sum_{j=1}^{n}\hat{\beta}^*_{zi}(\xi-\xi_i)^2U(\xi-\xi_i)$$
$$f_{z4}(\xi) = \xi^3+\sum_{j=1}^{n}\hat{\beta}^*_{zi}(\xi^3-3\xi_i^2\xi+2\xi_i^3)U(\xi-\xi_i)$$
$$f_{z5}(\xi) = p^{[4]}(\xi)+\sum_{i=1}^{n}\hat{\beta}^*_{zi}\left[p_z{}^{[4]}(\xi)-p_z{}^{[4]}(\xi_i)\right]U(\xi-\xi_i)-\sum_{i=1}^{n}\hat{\beta}^*_{zi}p_z{}^{[3]}(\xi_i)(\xi-\xi_i)U(\xi-\xi_i) \tag{A3}$$

and

$$f_{y3}(\xi) = \xi^2+\sum_{j=1}^{n}\hat{\beta}^*_{yi}(\xi-\xi_i)^2U(\xi-\xi_i)$$
$$f_{y4}(\xi) = \xi^3+\sum_{j=1}^{n}\hat{\beta}^*_{yi}(\xi^3-3\xi_i^2\xi+2\xi_i^3)U(\xi-\xi_i)$$
$$f_{y5}(\xi) = p^{[4]}(\xi)+\sum_{i=1}^{n}\hat{\beta}^*_{yi}\left[p_y{}^{[4]}(\xi)-p_y{}^{[4]}(\xi_i)\right]U(\xi-\xi_i)-\sum_{i=1}^{n}\hat{\beta}^*_{yi}p_y{}^{[3]}(\xi_i)(\xi-\xi_i)U(\xi-\xi_i) \tag{A4}$$

In Eqs. (A3) and (A4) the new parameters $\hat{\beta}^*_{zi}, \hat{\beta}^*_{yi}$ take into account both the in- and the of the out-of-plane influence of the discontinuity parameters and they are obtained in accordance to Eq. (6) as follows:

$$\hat{\beta}^*_{z,i} = \frac{\hat{\beta}_{z,i}}{1-\hat{\beta}_{z,i}} - \frac{\hat{\beta}_{z,i-1}}{1-\hat{\beta}_{z,i-1}}, \quad \hat{\beta}^*_{y,i} = \frac{\hat{\beta}_{y,i}}{1-\hat{\beta}_{y,i}} - \frac{\hat{\beta}_{y,i-1}}{1-\hat{\beta}_{y,i-1}} \tag{A5}$$

At this stage it is hence convenient to introduce the vectors $\hat{\boldsymbol{\beta}}^*_{\mathbf{z}} = [\hat{\beta}^*_{z1}\hat{\beta}^*_{z2}\ldots\hat{\beta}^*_{zn}]^T$, $\hat{\boldsymbol{\beta}}^*_{\mathbf{y}} = [\hat{\beta}^*_{y1}\hat{\beta}^*_{y2}\ldots\hat{\beta}^*_{yn}]^T$ and collect them in the vector $\hat{\boldsymbol{\beta}}^*$, accounting for the out-of-plane influence, as follows: $\hat{\boldsymbol{\beta}}^* = [\hat{\beta}^*_z\hat{\beta}^*_y]^T$.

According to the procedure proposed in the main body of the paper, the shape functions of the transversal displacements $u_z(\xi)$ and $u_y(\xi)$, characterising the out-of-plane SDB element, able to account for the occurrence of zones with discontinuous flexural stiffness due to plasticity, are obtained by the enforcement of the following nodal displacements and rotations:

$$\begin{aligned} &u_z(0) = q_1; \quad \varphi_y(0) = -u^I_z(0) = -q_2; \quad u_y(0) = q_3; \quad \varphi_z(0) = -u^I_y(0) = q_4; \\ &u_z(1) = q_5; \quad \varphi_y(1) = -u^I_z(1) = -q_6; \quad u_y(1) = q_7; \quad \varphi_z(1) = -u^I_y(1) = q_8 \end{aligned} \tag{A6}$$

Imposition of the boundary conditions in Eq. (A6) onto the closed form expression proposed in Eq. (A2), and its first derivative, in the x, z and x, y planes in turn, leads to the expressions of the beam axis transversal deflection in terms of nodal displacements and the external load function as follows:

$$\mathbf{u}(\xi;\boldsymbol{\xi}^{\mathbf{EI}},\hat{\boldsymbol{\beta}}^*) = \mathbf{N}(\xi;\boldsymbol{\xi}^{\mathbf{EI}},\hat{\boldsymbol{\beta}}^*)\cdot\mathbf{q}_e + \mathbf{u}_p(\xi;\boldsymbol{\xi}^{\mathbf{EI}},\hat{\boldsymbol{\beta}}^*) \tag{A7}$$

where

$$\begin{aligned} &\mathbf{u}(\xi;\boldsymbol{\xi}^{\mathbf{EI}},\hat{\boldsymbol{\beta}}^*) = \begin{bmatrix} u_z(\xi;\boldsymbol{\xi}^{\mathbf{EI}},\hat{\boldsymbol{\beta}}^*_{\mathbf{z}}) \\ u_y(\xi;\boldsymbol{\xi}^{\mathbf{EI}},\hat{\boldsymbol{\beta}}^*_{\mathbf{y}}) \end{bmatrix}; \quad \mathbf{u}_p(\xi;\boldsymbol{\xi}^{\mathbf{EI}},\hat{\boldsymbol{\beta}}^*) = \begin{bmatrix} u_{pz}(\xi;\boldsymbol{\xi}^{\mathbf{EI}},\hat{\boldsymbol{\beta}}^*_{\mathbf{z}}) \\ u_{py}(\xi;\boldsymbol{\xi}^{\mathbf{EI}},\hat{\boldsymbol{\beta}}^*_{\mathbf{y}}) \end{bmatrix} \\ &\mathbf{N}(\xi;\boldsymbol{\xi}^{\mathbf{EI}},\hat{\boldsymbol{\beta}}^*) = \begin{bmatrix} \mathbf{N}_z(\xi;\boldsymbol{\xi}^{\mathbf{EI}},\hat{\boldsymbol{\beta}}^*_{\mathbf{z}}) & \mathbf{0} \\ \mathbf{0} & \mathbf{N}_y(\xi;\boldsymbol{\xi}^{\mathbf{EI}},\hat{\boldsymbol{\beta}}^*_{\mathbf{y}}) \end{bmatrix}; \\ &\mathbf{N}_z(\xi;\boldsymbol{\xi}^{\mathbf{EI}},\hat{\boldsymbol{\beta}}^*_{\mathbf{z}}) = \left[N_{z,1}(\xi;\boldsymbol{\xi}^{\mathbf{EI}},\hat{\boldsymbol{\beta}}^*_{\mathbf{z}})N_{z,2}(\xi;\boldsymbol{\xi}^{\mathbf{EI}},\hat{\boldsymbol{\beta}}^*_{\mathbf{z}})N_{z,3}(\xi;\boldsymbol{\xi}^{\mathbf{EI}},\hat{\boldsymbol{\beta}}^*_{\mathbf{z}})N_{z,4}(\xi;\boldsymbol{\xi}^{\mathbf{EI}},\hat{\boldsymbol{\beta}}^*_{\mathbf{z}})\right]; \\ &\mathbf{N}_y(\xi;\boldsymbol{\xi}^{\mathbf{EI}},\hat{\boldsymbol{\beta}}^*_{\mathbf{y}}) = \left[N_{y,1}(\xi;\boldsymbol{\xi}^{\mathbf{EI}},\hat{\boldsymbol{\beta}}^*_{\mathbf{y}})N_{y,2}(\xi;\boldsymbol{\xi}^{\mathbf{EI}},\hat{\boldsymbol{\beta}}^*_{\mathbf{y}})N_{y,3}(\xi;\boldsymbol{\xi}^{\mathbf{EI}},\hat{\boldsymbol{\beta}}^*_{\mathbf{y}})N_{y,4}(\xi;\boldsymbol{\xi}^{\mathbf{EI}},\hat{\boldsymbol{\beta}}^*_{\mathbf{y}})\right] \end{aligned} \tag{A8}$$

The functions $N_{z,j}(\xi;\boldsymbol{\xi}^{\mathbf{EI}},\hat{\boldsymbol{\beta}}^*_{\mathbf{z}}), N_{y,j}(\xi;\boldsymbol{\xi}^{\mathbf{EI}},\hat{\boldsymbol{\beta}}^*_{\mathbf{y}}),\ j = 1,\ldots,4$, appearing in Eqs. (A7) and (A8) are the displacement shape functions, collected in the matrix $\mathbf{N}(\xi;\boldsymbol{\xi}^{\mathbf{EI}},\hat{\boldsymbol{\beta}}^*)$, dependent on the abscissas and intensity of the flexural stiffness discontinuities collected in the vectors $\boldsymbol{\xi}^{\mathbf{EI}}, \hat{\boldsymbol{\beta}}^*$, respectively. Moreover, the vector $\mathbf{u}_p(\xi;\boldsymbol{\xi}^{\mathbf{EI}},\hat{\boldsymbol{\beta}}^*)$ in Eq. (A7), contains the contributions of the external loads $p_z(\xi)$, $p_y(\xi)$ to the transversal displacements.

The explicit expressions of the shape functions $N_{z,j}(\xi;\boldsymbol{\xi}^{\mathbf{EI}},\hat{\boldsymbol{\beta}}^*_{\mathbf{z}}), N_{y,j}(\xi;\boldsymbol{\xi}^{\mathbf{EI}},\hat{\boldsymbol{\beta}}^*_{\mathbf{y}}),\ j = 1,\ldots,4$ of the transversal displacements $u_z(\xi)$ and $u_y(\xi)$ of the beam axis, in view of Eq. (A2), can be written as follows:

$$\begin{aligned} &N_{z,j}(\xi;\boldsymbol{\xi}^{\mathbf{EI}},\hat{\boldsymbol{\beta}}^*_{\mathbf{z}}) = {}^jC_{z1} + {}^jC_{z2}\xi + {}^jC_{z3}f_{z3}(\xi;\xi_i,\hat{\beta}^*_{z,i}) + {}^jC_{z4}f_{z4}(\xi;\xi_i,\hat{\beta}^*_{z,i}), \\ &N_{y,j}(\xi;\boldsymbol{\xi}^{\mathbf{EI}},\hat{\boldsymbol{\beta}}^*_{\mathbf{y}}) = {}^jC_{y1} + {}^jC_{y2}\xi + {}^jC_{y3}f_{y3}(\xi;\xi_i,\hat{\beta}^*_{y,i}) + {}^jC_{y4}f_{y4}(\xi;\xi_i,\hat{\beta}^*_{y,i}), \\ &i = 1,\ldots,n, \quad j = 1,\ldots,4 \end{aligned} \tag{A9}$$

where $f_{z3}(\xi;\xi_i,\hat{\beta}^*_{z,i}), f_{z4}(\xi;\xi_i,\hat{\beta}^*_{z,i})$ and $f_{y3}(\xi;\xi_i,\hat{\beta}^*_{y,i}), f_{y4}(\xi;\xi_i,\hat{\beta}^*_{y,i})$ are defined in Eqs. (A3) and (A4), respectively.

Furthermore, the constants ${}^jC_{z1}, {}^jC_{z2}, {}^jC_{z3}, {}^jC_{z4}$ and ${}^jC_{y1}, {}^jC_{y2}, {}^jC_{y3}, {}^jC_{y4}$ (with j = 1, ..., 4) in Eq. (A9) can be inferred by Eq. (12) with the adoption of $f_{z3}(\xi;\xi_i,\hat{\beta}^*_{z,i}), f_{z4}(\xi;\xi_i,\hat{\beta}^*_{z,i})$ and $f_{y3}(\xi;\xi_i,\hat{\beta}^*_{y,i}), f_{y4}(\xi;\xi_i,\hat{\beta}^*_{y,i})$ given Eqs. (A3) and (A4), respectively, in their definition. The terms $u_{pz}(\xi;\boldsymbol{\xi}^{\mathbf{EI}},\hat{\boldsymbol{\beta}}^*), u_{py}(\xi;\boldsymbol{\xi}^{\mathbf{EI}},\hat{\boldsymbol{\beta}}^*)$ related to the contribution of the external load can be inferred by the expressions in Eqs. (13) and (14) with the adoption of $f_{z3}(\xi)$, $f_{z4}(\xi)$, $f_{z5}(\xi)$ and $f_{y3}(\xi)$, $f_{y4}(\xi)$, $f_{y5}(\xi)$ respectively, in their definition.

Considering the out-of-plane behaviour, the curvatures $\chi_z(\xi;\boldsymbol{\xi}^{\mathbf{EI}},\hat{\boldsymbol{\beta}}^*_{\mathbf{z}})$ and $\chi_y(\xi;\boldsymbol{\xi}^{\mathbf{EI}},\hat{\boldsymbol{\beta}}^*_{\mathbf{z}})$ of the beam element can be expressed in terms of nodal displacements and distributed external forces as follows:

$$\boldsymbol{\chi}(\xi;\boldsymbol{\xi}^{\mathbf{EI}},\hat{\boldsymbol{\beta}}^*_{\mathbf{z}}) = \begin{bmatrix} \chi_y(\xi;\boldsymbol{\xi}^{\mathbf{EI}},\hat{\boldsymbol{\beta}}^*_{\mathbf{z}}) \\ \chi_z(\xi;\boldsymbol{\xi}^{\mathbf{EI}},\hat{\boldsymbol{\beta}}^*_{\mathbf{y}}) \end{bmatrix} = \mathbf{B}(\xi;\boldsymbol{\xi}^{\mathbf{EI}},\hat{\boldsymbol{\beta}}^*_{\mathbf{z}})\cdot\mathbf{q}_e - \mathbf{u}^{II}_p\left(\xi;\boldsymbol{\xi}^{\mathbf{EI}},\hat{\boldsymbol{\beta}}^*_{\mathbf{z}}\right) \tag{A10}$$

where $\mathbf{B}(\xi;\boldsymbol{\xi}^{\mathbf{EI}},\hat{\boldsymbol{\beta}}^*)$, defined as follows:

$$\mathbf{B}(\xi;\boldsymbol{\xi}^{\mathbf{EI}},\hat{\boldsymbol{\beta}}^{*})=\begin{bmatrix}-\mathbf{N}_z^{II}(\xi;\boldsymbol{\xi}^{\mathbf{EI}},\hat{\boldsymbol{\beta}}_{\mathbf{z}}^{*}) & \mathbf{0}\\ \mathbf{0} & -\mathbf{N}_y^{II}(\xi;\boldsymbol{\xi}^{\mathbf{EI}},\hat{\boldsymbol{\beta}}_{\mathbf{y}}^{*})\end{bmatrix} \tag{A11}$$

is the matrix collecting the curvature shape functions obtained as second derivatives of the transversal displacement shape functions containing the effect of the discontinuities.

In the presented out-of-plane beam element the normalised bending moments, collected in the bending moment vector $\mathbf{M}(\xi;\boldsymbol{\xi}^{\mathbf{EI}},\hat{\boldsymbol{\beta}}_{\mathbf{z}}^{*})=[M_y(\xi;\boldsymbol{\xi}^{\mathbf{EI}},\hat{\boldsymbol{\beta}}_{\mathbf{z}}^{*})M_z(\xi;\boldsymbol{\xi}^{\mathbf{EI}},\hat{\boldsymbol{\beta}}_{\mathbf{y}}^{*})]^T$, are related to the curvature vector by means of the following relationship:

$$\mathbf{M}(\xi;\boldsymbol{\xi}^{\mathbf{EI}},\boldsymbol{\beta},\hat{\boldsymbol{\beta}}^{*})=\mathbf{k}(\xi;\boldsymbol{\xi}^{\mathbf{EI}},\boldsymbol{\beta})\ \chi(\xi;\boldsymbol{\xi}^{\mathbf{EI}},\hat{\boldsymbol{\beta}}^{*})=\begin{bmatrix}k_{zz}(\xi;\boldsymbol{\xi}^{\mathbf{EI}},\boldsymbol{\beta}_{\mathbf{z}}) & k_{zy}(\xi;\boldsymbol{\xi}^{\mathbf{EI}},\boldsymbol{\beta}_{\mathbf{y}})\\ k_{yz}(\xi;\boldsymbol{\xi}^{\mathbf{EI}},\boldsymbol{\beta}_{\mathbf{z}}) & k_{yy}(\xi;\boldsymbol{\xi}^{\mathbf{EI}},\boldsymbol{\beta}_{\mathbf{y}})\end{bmatrix}\begin{bmatrix}\chi_y(\xi;\boldsymbol{\xi}^{\mathbf{EI}},\hat{\boldsymbol{\beta}}_{\mathbf{z}})\\ \chi_z(\xi;\boldsymbol{\xi}^{\mathbf{EI}},\hat{\boldsymbol{\beta}}_{\mathbf{y}})\end{bmatrix} \tag{A12}$$

where the components of the normalised cross section flexural stiffness matrix $\mathbf{k}(\xi;\ \xi^{\mathrm{EI}},\ \boldsymbol{\beta})$, according to the model introduced in Eq. (A1), are defined as follows:

$$k_{zz}(\xi;\boldsymbol{\xi}^{\mathbf{EI}},\boldsymbol{\beta}_{\mathbf{z}})=1-\sum_{i=1}^{n}(\beta_{z,i}-\beta_{z,i-1})U(\xi-\xi_i) \tag{A13}$$

$$k_{zy}(\xi;\boldsymbol{\xi}^{\mathbf{EI}},\boldsymbol{\beta}_{\mathbf{y}})=\kappa_z\left[1-\sum_{i=1}^{n}(\beta_{y,i}-\beta_{y,i-1})U(\xi-\xi_i)\right] \tag{A13}$$

$$k_{yz}(\xi;\boldsymbol{\xi}^{\mathbf{EI}},\boldsymbol{\beta}_{\mathbf{z}})=\kappa_y\left[1-\sum_{i=1}^{n}(\beta_{z,i}-\beta_{z,i-1})U(\xi-\xi_i)\right] \tag{A13}$$

$$k_{yy}(\xi;\boldsymbol{\xi}^{\mathbf{EI}},\boldsymbol{\beta}_{\mathbf{y}})=1-\sum_{i=1}^{n}(\beta_{y,i}-\beta_{y,i-1})U(\xi-\xi_i) \tag{A13}$$

The non linear variation of the flexural stiffness, as plastic deformations occur, will be explicitly formulated by updating the vectors β_z, β_y, in the relevant beam segments identified by the vector ξ^{EI}.

The relationship between the force and displacement element nodal vectors $\mathbf{Q}_e$ and q_e is:

$$\mathbf{Q}_e=\mathbf{K_e}(\boldsymbol{\xi}^{\mathbf{EI}},\boldsymbol{\beta},\hat{\boldsymbol{\beta}}^{*})\cdot\mathbf{q}_e \tag{A14}$$

where $\mathbf{K_e}(\boldsymbol{\xi}^{\mathbf{EI}},\boldsymbol{\beta},\hat{\boldsymbol{\beta}}^{*})$ is the element stiffness matrix, dependent on the current state of the element by means of the plastic intensity parameter vectors $\boldsymbol{\beta},\hat{\boldsymbol{\beta}}^{*}$ and the plastic segment extension vector ξ^{EI}, defined as follows:

$$\mathbf{K_e}(\boldsymbol{\xi}^{\mathbf{EI}},\boldsymbol{\beta},\hat{\boldsymbol{\beta}}^{*})=\int_0^1\mathbf{B}^{\mathbf{T}}(\xi;\boldsymbol{\xi}^{\mathbf{EI}},\hat{\boldsymbol{\beta}}^{*})\mathbf{k}(\xi;\boldsymbol{\xi}^{\mathbf{EI}},\boldsymbol{\beta})\mathbf{B}(\xi;\boldsymbol{\xi}^{\mathbf{EI}},\hat{\boldsymbol{\beta}}^{*})\,d\xi \tag{A15}$$

and, according to the Gauss integration scheme, the element stiffness matrix is evaluated as follows:

$$\mathbf{K_e}(\boldsymbol{\xi}^{\mathbf{EI}},\boldsymbol{\beta},\hat{\boldsymbol{\beta}}^{*})\approx\sum_{r=1}^{N}\mathbf{B}^{\mathbf{T}}(\xi_r^G;\boldsymbol{\xi}^{\mathbf{EI}},\hat{\boldsymbol{\beta}}^{*})\mathbf{k}(\xi_r^G;\boldsymbol{\xi}^{\mathbf{EI}},\boldsymbol{\beta})\mathbf{B}(\xi_r^G;\boldsymbol{\xi}^{\mathbf{EI}},\hat{\boldsymbol{\beta}}^{*})\,w_r \tag{A16}$$

The incremental plastic constitutive law can be formulated according to the associative plasticity hypothesis and is integrated at the controlled Gauss sections ξ_r^G, $r=1,\dots,N$, by adopting a yield function for the cross section. Only as a matter of example, for a nonlinear kinematic hardening type of behaviour, the yield function may assume the following form:

$$\Phi=\left(\frac{M_y-H_{ky}(\chi_y^p)\chi_y^p}{M_{yE}}\right)^{\alpha}+\left(\frac{M_z-H_{kz}(\chi_y^p)\chi_z^p}{M_{zE}}\right)^{\alpha}-1=0 \tag{A17}$$

where M_{zE}, M_{yE} are the limit elastic bending moments, χ_z^p,χ_y^p are the plastic curvature components and $H_{kz}(\chi_z^p),H_{ky}(\chi_y^p)$ are the kinematic hardening moduli to be specified according to the desired nonlinear behaviour. Eq. (A17) represents a yield surface in the M_z, M_y plane containing all the admissible stress points.

According to the strategy of the Newton–Raphson iterative algorithm, the integration procedure of the incremental holonomic plastic constitutive laws at each Gauss point is composed of an elastic predictor phase and, for those points outside the yield surface $\Phi>0$ in Eq. (A12), a successive plastic corrector phase implying a return onto the yield surface $\Phi=0$ to provide the updated bending moments. The return algorithms available in the literature differ from each other according to the chosen path followed by the plastic deformations into the incremental step [48,49]. According to the chosen return algorithm, the relationship between the bending moment and the deformation increments provides the so called updated "consistent tangent matrix" of the relevant Gauss section to be adopted for $\mathbf{k}(\xi_r^G;\boldsymbol{\xi}^{\mathbf{EI}},\boldsymbol{\beta})$ in Eq. (A16) [50,51].

Since the above steps are standard and well established in the literature have been only very briefly summarised. However, it has to be pointed out that the updating procedure during the plastic analysis is developed as follows:

(i) once the components k_{zz}, k_{zy}, k_{yz}, k_{yy} of the stiffness matrix are updated at each Gauss point with the consistent tangent matrix, the discontinuity parameters $\beta_{z,i}$, $\beta_{y,i}$ and the constants κ_z, κ_y are also updated by means of Eq. (A13) to provide $\hat{\beta}_{z,i} = \beta_{z,i} + \kappa_z \beta_{y,i}$ and $\hat{\beta}_{y,i} = \beta_{y,i} + \kappa_y \beta_{z,i}$, $i = 1, \ldots, n$;

(ii) the updated vector $\hat{\boldsymbol{\beta}}^*$ at each Gauss section is obtained by Eq. (A5);

(iii) the new SDB beam element requires the updating of the curvature shape function matrix $\mathbf{B}(\xi; \boldsymbol{\xi}^{\mathbf{EI}}, \hat{\boldsymbol{\beta}}^*)$, provided by Eq. (A11), depending on the development of the plastic curvature components along the beam axis and, finally, the stiffness matrix $\mathbf{K_e}(\boldsymbol{\xi}^{\mathbf{EI}}, \boldsymbol{\beta}, \hat{\boldsymbol{\beta}}^*)$ given by Eq. (A16), can also be updated.

References

[1] M.A. Crisfield, Finite Elements and Solution Procedures For Structural Analysis, vol. 1, Linear Analysis, Pineridge Press, Swansea, UK, 1986.
[2] M.A. Crisfield, Non-Linear Finite Element Analysis of Solids and Structures, 1, John Wiley & Sons, Chichester, UK, 1991.
[3] M.A. Crisfield, Non-Linear Finite Element Analysis of Solids and Structures, vol. 2, John Wiley & Sons, (1997) Chichester, UK.
[4] O.C. Zienkiewicz, R.L. Taylor, The Finite Element Method: The Basis, vol. 1. 5th edn., Butterworth-Heinemann, (2000) Oxford, UK.
[5] O.C. Zienkiewicz, R.L. Taylor, The Finite Element Method: Solid Mechanics, 2, 5th edn, Butterworth-Heinemann, Oxford, UK, 2000.
[6] K.J. Bathe, Finite Element Procedures, Prentice Hall, Englewood Cliffs, 1996 NJ, USA.
[7] V. Ciampi, L. Carlesimo, A nonlinear beam element for seismic analysis of structures, in: Proceedings of the 8th European Conference on Earthquake Engineering, Lisbon, Portugal, 1986, pp. 73–80.
[8] I. Carol, J. Murcia, Nonlinear time-dependent analysis of planar frames using an 'exact' formulation – I: Theory, Comput. Struct. 33 (1989) 79–87.
[9] F.F. Taucer, E. Spacone, F.C. Filippou, A Fiber Beam-Column Method for Seismic Response Analysis of Reinforced Concrete Structures, Report No. UCB/EERCC-91/17 Earthquake Engineering Research Center, College of Engineering, University of California, Berkeley (1991).
[10] E. Spacone, V. Ciampi, F.C. Filippou, A Beam Element for Seismic Damage Analysis. Report No. UCB/EERCC-92/07 Earthquake Engineering Research Center, College of Engineering, University of California, Berkeley (1992).
[11] E. Spacone, V. Ciampi, F.C. Filippou, Mixed formulation of nonlinear beam finite element, Comput. Struct. 58 (1) (1996) 71–83.
[12] A. Neuenhofer, F.C. Filippou, Evaluation of nonlinear frame finite element models, J. Struct. Eng. (ASCE) 123 (7) (1997) 958–956.
[13] E. Spacone, F.C. Filippou, F.F. Taucer, Fiber beam-column model for non-linear analysis of r/c frames: Part I. Formulation, Earthq. Eng. Struct. Dyn. 25 (1996) 711–725.
[14] E. Spacone, F.C. Filippou, F.F. Taucer, Fiber beam-column model for non-linear analysis of r/c frames: Part II. Applications, Earthq. Eng. Struct. Dyn. 25 (1996) 727–742.
[15] S. Kaba, S.A. Mahin, Refined Modeling of Reinforced Concrete Columns for Seismic Analysis. Report No. UCB/EERC-84/03, Earthquake Engineering Research Center, University of California, Berkeley, CA, USA (1984).
[16] C. Zeris, S.A. Mahin, Analysis of reinforced concrete beam-columns under uniaxial excitation, J. Struct. Eng. (ASCE) 114 (ST4) (1988) 804–820.
[17] A. Neuenhofer, F.C. Filippou, Geometrically nonlinear flexibility-based frame finite element, J. Struct. Eng. (ASCE) 124 (6) (1998) 704–711.
[18] J. Backlund, Large deflection analysis of elasto-plastic beams and frames, Int. J. Mech. Sci. 18 (1976) 269–277.
[19] A. Ayoub, F.C. Filippou, Mixed formulation of bond-slip problems under cyclic loads, J. Struct. Eng. ASCE 125 (ST6) (1999) 661–671.
[20] A. Ayoub, F.C. Filippou, Mixed formulation of nonlinear steel-concrete composite beam element, J. Struct. Eng. ASCE 126 (2000) 371–381.
[21] K.D. Hjelmstad, E. Taciroglu, Mixed methods and flexibility approaches for non-linear frame analysis, J. Contruct. Steel Res. 58 (2002) 967–993.
[22] S. Limkatanyu, E. Spacone, Reinforced concrete frame element with bond interfaces I: Displacement-based, Force-based, and mixed formulations, J. Struct. Eng. ASCE 128 (ST3) (2002) 346–355.
[23] R.L. Taylor, F.C. Filippou, A. Saritas, F. Auricchio, A mixed finite element method for beam and frame problems, Comput. Mech. 31 (2003) 192–203.
[24] B.A. Izzudin, A.S. Elnashai, Adaptive space frame analysis: part I, a plastic hinge approach, Struct. Build. 99 (3) (1993) 303–316.
[25] B.A. Izzudin, A.S. Elnashai, Adaptive space frame analysis: part II, a distributed plasticity approach, Struct. Build. 99 (3) (1993) 317–326.
[26] B.A. Izzudin, C.G. Karayannis, A.S. Elnashai, Advanced nonlinear formulation for reinforced concrete beam-columns, J. Struct. Eng. (ASCE) 120 (10) (1994) 2913–2934.
[27] C.G. Karayannis, B.A. Izzudin, A.S. Elnashai, Application of adaptive analysis to reinforced concrete frames, J. Struct. Eng. (ASCE) 120 (10) (1994) 2934–2957.
[28] B.A. Izzudin, A.S. Elnashai, ADAPTIC: A Program for the Adaptive dynamic analysis of space frames. Report No. ESEE-89/7, Imperial College, London, England (1989).
[29] M. Mahasuverachai, G.H. Powell, Inelastic analysis of piping and tubular structures, Report No. UCB/EERC-82/27, Earthquake Engineering Research Center, University of California, Berkeley, CA, USA (1982).
[30] B. Stock, M. Halilovic, Analytical solutions in elasto-plastic bending of beams with rectangular cross section, Appl. Math. Mod. 33 (2009) 1749–1760.
[31] B. Biondi, S. Caddemi, Closed form solutions of Euler-Bernoulli beams with singularities, Int. J. Solids Struct. 42 (2005) 3027–3044.
[32] B. Biondi, S. Caddemi, Euler-Bernoulli beams with multiple singularities in the flexural stiffness, Eur. J. Mech. A/Solids 26 (5) (2007) 789–809.
[33] Q.S. Li, Free vibration analysis of non-uniform beams with an arbitrary number of cracks and concentrated masses, J. Sound Vib. 252 (3) (2002) 509–525.
[34] Q.S. Li, Buckling of an elastically restrained multi-step non-uniform beam with multiple cracks, Arch. Appl. Mech. 72 (2002) 522–535.
[35] A. Yavari, S. Sarkani, On applications of generalised functions to the analysis of Euler–Bernoulli beam-columns with jump discontinuities, Int. J. Mech. Sci. 43 (2001) 1543–1562.
[36] A. Yavari, S. Sarkani, E.T. Moyer, On applications of generalised functions to beam bending problems, Int. J. Solids Struct. 37 (2000) 5675–5705.
[37] A. Yavari, S. Sarkani, J.N. Reddy, On nonuniform Euler–Bernoulli and Timoshenko beams with jump discontinuities: application of distribution theory, Int. J. Solids Struct. 38 (2001) 8389–8406.
[38] A. Yavari, S. Sarkani, J.N. Reddy, Generalised solutions of beams with jump discontinuities on elastic foundations, Arch. Appl. Mech. 71 (9) (2001) 625–639.
[39] J. Wang, P. Qiao, Vibration of beams with arbitrary discontinuities and boundary conditions, J. Sound Vib. 308 (2007) 12–27.
[40] S. Caddemi, I. Caliò, Exact closed-form solution for the vibration modes of the Euler-Bernoulli beam multiple open cracks, J. Sound Vib. 327 (2009) 473–489.
[41] S. Caddemi, I. Caliò, The exact explicit dynamic stiffness matrix of multi-cracked Euler-Bernoulli beam and application to damaged frame structures, J. Sound Vib. 332 (2013) 3049–3063.
[42] S. Caddemi, I. Caliò, F. Cannizzaro, Closed-form solutions for stepped Timoshenko beams with internal singularities and along-axis external supports, Arch. Appl. Mech. 83 (2013) 559–577.
[43] S. Caddemi, I. Caliò, F. Cannizzaro, D. Rapicavoli, A novel beam finite element with singularities for the dynamic analysis of discontinuous frames, Arch. Appl. Mech. 83 (10) (2013) 1451–1468.
[44] P.E. Mergos, A.J. Kappos, A distributed shear and flexural flexibility model with shear–flexure interaction for R/C members subjected to seismic loading, Earthq. Engng. Struct. Dyn 37 (2008) 1349–1370.
[45] P.E. Mergos, A.J. Kappos, Seismic damage analysis including inelastic shear–flexure interaction, Bull. Earthq. Eng. 8 (2010) 27.

[46] P. Ceresa, L. Petrini, R. Pinho, Flexure-shear fiber beam-column elements for modeling frame structures under seismic loading — State of the art, J. Earthq. Eng. 11 (2007) 46–88.
[47] P. Ceresa, L. Petrini, R. Pinho, R. Sousa, A fibre flexure–shear model for seismic analysis of RC-framed structures, Earthq. Eng. Struct. Dyn. 38 (2009) 565–586.
[48] L.J. Recontre, S. Caddemi, J.B. Martin, The relationship between the generalised mid-point and trapezoidal rules in incremental elasto-plasticity, Comput. Meth. Appl. Mech. Eng. 96 (1992) 201–212.
[49] S. Caddemi, Computational Aspects of the integration of the Von Mises linear hardening constitutive laws, Int. J. Plast. 10 (1994) 935–956.
[50] J.C. Simo, R.L. Taylor, Consistent tangent operators for rate-independent elastoplasticity, Comput. Meth. Appl. Mech. Eng. 48 (1985) 101–118.
[51] S. Caddemi, J.B. Martin, Convergence of the Newton-Raphson algorithm in elastic-plastic incremental analysis, Int. J. Numer. Meth. Eng. 31 (1991) 177–191.